OAK RIDGE NATIONAL LABORATORY
operated by
UNION CARBIDE CORPORATION
NUCLEAR DIVISION
for the
U.S. ATOMIC ENERGY COMMISSION

UNION CARBIDE

ORNL - TM - 1630
NASA-CR-72070

46

NASA TUNGSTEN REACTOR RADIATION CHEMISTRY STUDIES

FINAL REPORT

G.H. Jenks, H.C. Savage, and E.G. Bohlmann

FACILITY FORM 602

N66 38496
(ACCESSION NUMBER)
(THRU)
120
(PAGES)
1
(CODE)
CR-72070
(NASA CR OR TMX OR AD NUMBER)
06
(CATEGORY)

GPO PRICE $
CFSTI PRICE(S) $
Hard copy (HC) 3.00
Microfiche (MF) 1.00

ff 653 July 65

NOTICE This document contains information of
and was prepared primarily for internal use at the Oak Ridge National
Laboratory. It is subject to revision or correction and therefore does
not represent a final report.

ORNL-TM-1630
NASA-CR-72070

NASA TUNGSTEN REACTOR RADIATION CHEMISTRY STUDIES

FINAL REPORT

G.H. Jenks, H. C. Savage, and E. G. Bohlmann

Technical Management
NASA LEWIS RESEARCH CENTER
CLEVELAND, OHIO
REACTOR APPLICATIONS BRANCH
NUCLEAR SYSTEMS DIVISION
H. W. Davison

OCTOBER 1966

"This program at Oak Ridge National Laboratory was funded by the National Aeronautics and Space Administration-Lewis Research Center under an Interagency Agreement with the Atomic Energy Commission."

OAK RIDGE NATIONAL LABORATORY
Oak Ridge, Tennessee
Operated by
UNION CARBIDE CORPORATION
for the
U. S. ATOMIC ENERGY COMMISSION

SUMMARY

Experimental investigations were made of the stability of $CdSO_4$ solutions under electron irradiation.

The experimental conditions studied were as follows:

Solution composition - 0.02 and 0.067 M $CdSO_4$ in water.
Temperature - 60 to 120°C range.
Radiation Intensity - 73 and 145 w per cc of solution.
Container - Zircaloy-2 with titanium filter.
Agitation - static solution.
Surface area to volume ratio - 61 cm^2/cc.

Small amounts of Cd were lost during 30 min irradiations at each tested combination of the above set of conditions. With 0.02 M $CdSO_4$ solutions, the loss at 120°C and 145 w per cc was 5.0% ± 3.4% error at 80% confidence. The loss at 77°C was 3.3% ± 2.8% and that at 77°C and 73 w per cc was 2.0 ± 2.7%. One experiment with 0.02 M $CdSO_4$ and H_2SO_4, pH 2, indicated negligible loss.

With 0.06 M $CdSO_4$, the loss at 60°C and 145 w per cc was 1.5% ± 1.0%. At 120°C, the best indication was about 4% loss. The results of experiments with 5- and 50-min irradiations of 0.067 M $CdSO_4$ at 60°C and 145 w per cc indicated that the amount of Cd lost was greatest at the longer time.

Experimental information on recovery of the separated Cd after irradiation indicated that the rates of redissolution are slow.

Considerations of these results and of theory suggest that Cd metal is formed under irradiation and that this separates as relatively insoluble material by agglomeration or by plating on solid surfaces. Additional experimental investigation of effects of agitation and of surface area to volume

ratios would be required to predict the effects of radiation on stability in a reactor in which these parameters differ from those in the present experiments.

Equipment for this experimental work was designed and developed. Also design and development work was done on a system which could be used to study effects of irradiation on stability in a dynamic system. The planned dynamic experiment was to be conducted with a small, high speed (35,000 rpm), centrifugal pump with which solution was to be circulated thru a small bore tube forming a loop in front of the cover plate of the pump. The entire solution inventory was to be irradiated continuously. The purpose of the tube was to provide a channel in which film conditions could be made comparable to those in the Tungsten Water Moderated Reactor. A substantial part of the development work was concerned with (1) establishing experimental arrangements in which uniform power densities of about 150 w per cc would prevail during electron bombardment using an available Van de Graaff accelerator, and (2) establishing the relationship between electron beam current and power density. Solution dosimetery and beam current measurements were employed.

Table of Contents

1. Introduction

Poison control solutions of $CdSO_4$ are being considered by the NASA Lewis Research Center for possible use in the NASA Tungsten Water-Moderated Reactor (TWMR). Information regarding the effects of irradiations on the stability of these solutions toward loss of Cd was needed in evaluations of this poison control system. We have planned and developed experiments to test $CdSO_4$ solutions under electron irradiation with intensities and other conditions such that they either simulate those in the reactor or provide a severe test of precipitation of Cd metal or compounds from the bulk of solution in the reactor. Two principal types of experiments were planned: those in which the solution would be static during irradiation and those in which the solution would be circulated to produce film conditions comparable to those in the reactor. The static system was completed and used in tests of solution stability at several different sets of conditions. The dynamic system was designed, and the design was shown to be feasible and adequate by component testing. The final dynamic system was not constructed.

Experiments were conducted on 0.02 and 0.067 M $CdSO_4$ in the temperature range 60 to 120°C and in the radiation intensity range of 75 to 150 w per cc of solution. The pH was that of the neutral salt in all but one experiment with 0.02 M $CdSO_4$ which was adjusted to pH-2 with H_2SO_4. The test conditions studied were limited to these because of the expiration time available for experimentation.

2 Bases for Experiment Design

2.1 Introduction

As indicated above, the basic criterion for the design of experiments was that experimental conditions either simulate those in the reactor or provide a severe test of solution stability in the reactor. Radiation effects which were tested were those which might originate from changes in the solution. Radiation effects which might originate from changes in the adsorption properties of the container material under neutron irradiation were not tested.* The use of fast electrons rather than reactor radiations in these experiments was justified on the basis of theoretical considerations of the course of radiolysis under electron and reactor radiations. It was also justified from the standpoints of readily available high radiation intensities and relative simplicity of experiments. These and other considerations relating to the design were reported[1] previously and are summarized below.

Reference information on a $CdSO_4$ poison control system for TWMR is listed in Table 1.

2.2 Theoretical

2.2.1 Radiolytic Reactions in $CdSO_4$ Solutions and Instability in Bulk of Solutions.

a. General

Radiation effects on solutes such as $CdSO_4$ in dilute aqueous solution are brought about by reactions between the solute and the radiolytic products of water. These products include oxidizing and reducing radicals (e^-_{aq}, H, OH, and HO_2) as well as molecular products (H_2, H_2O_2, and O_2). Although the hydrogen atom, H, does not react with Cd^{+2}, it is known that the hydrated electron, e^-_{aq}, reacts at a rapid rate, and the product is thought to be Cd^{+1} (Table 2, reaction 33).[2,3] The fate of the Cd^{+1} in a given solution is uncertain be-

---

*We do not imply that any such effects are likely to be important. However, additional considerations of this possibility should be made.

Table 1. Reference Information for $CdSO_4$ Poison-Control System in TWMR

Parameter	Description or Value
Solution Composition	
Solvent	H_2O
$CdSO_4$	.01 to 0.1 M
H_2SO_4	[a]
Gas content	[b]
Container	Zircaloy-2
Flow rate	40 ft per sec
Temperature	60 to 120°C
Radiation	
γ-rays	50 w/cc
fast neutrons	100 w/cc
Time	[c]

---

[a] Sulfuric acid additions were considered a possibility.

[b] Radiolytic gas and corrosion hydrogen would presumably be present but the concentrations were unknown.

[c] Intermittent irradiation with pulse times of a few sec and total times of several min.

cause the rate constants for possibly important reactions of this species are unknown. Reactions which were thought to be of possible importance in TWMR are included in Table 2. Only Reaction 48 could plausibly affect the stability of Cd in the bulk of solution in a steady-state since Cd-metal is produced,* and the rate of oxidation of the metal could be relatively slow. The other reactions result in the reoxidation of Cd^{+1} to Cd^{+2}. If the reaction rates were such that the oxidation reactions predominate strongly over reaction 48, no significant amount of Cd-metal would be expected. Significant reduction effects stemming from reactions with the sulfate seem unlikely.[6]

The results of calculations[1] of steady-state concentrations of radiolytic species in which reactions 48 and 25 were assumed to occur along with the usual radiolytic reactions in water led to the conclusion that for certain plausible sets of rate constants an appreciable fraction** of the cation would exist in the reduced form. This led to the further conclusions that the formation of Cd-metal in TWMR could not be excluded on the basis of available information, and that experiments would be required to determine stability under irradiation.

b. Intermittent vs continuous irradiation

The radiolysis of solutions in which active intermediates are formed at appreciable concentrations may differ between intermittent and continuous irradiation. Theoretical considerations[1] indicated that continuous irradiation for periods of at least several seconds would most closely duplicate expected behavior in TWMR.

---

*Others[2,4,5] have observed that metallic Cd is formed during electron irradiations of $CdSO_4$ solutions, and they suggested[2] that reaction 48 was a possible explanation.

**The calculations employed 0.001 M $CdSO_4$ solution, and the calculated concentrations of Cd^{+1} ranged up to 50% or more of the Cd in solution.

Table 2. Reactions of Possible Importance in Radiolysis of $CdSO_4$ Solutions

Reaction No[a]	Reaction	Rate Constant near 25°C (sec^{-1},m^{-1},ℓ)
33	$Cd^{+2} + e^-_{aq} \rightarrow Cd^{+1}$	5.8×10^{10}
48	$Cd^{+1} + Cd^{+1} \rightarrow Cd^o + Cd^{+2}$	------
25	$Cd^{+1} + OH \rightarrow Cd^{+2} + OH^-$	------
36, 37, 38	$Cd^{+1} + (H^+, HO_2, H_2O_2) \rightarrow Cd^{+2}+$	------

[a] Reaction numbers are those in reference 1.

c. Effect of (H^+)

The addition of acid would be expected to reduce the possibility of radiation effects on stability because of the reaction,

$$e^-_{aq} + H^+ \rightarrow H. \quad (k_{22} = 2.3 \times 10^{10}\ sec^{-1}, m^{-1}, \ell).^7 \qquad (2)$$

As mentioned above, the hydrogen atom, H, probably does not react with Cd^{+2}.[2] In order that hydrogen ions exercise an appreciable effect by this mechanism the concentration must be about $2.5(Cd^{+2})$*

The addition of acid may also improve solution stability by increasing the rate of oxidation by H^+ of Cd^{+1} and Cd^o to Cd^{+2}. The probability that this mechanism would be effective could not be assessed because the reaction rate constants are unknown.

d. Hydrogen in solution

The steady-state concentrations of H_2O_2 and HO_2 are reduced by the addition of excess H_2.[1] Accordingly, if these species are important in oxidizing Cd^{+1}, the addition of H_2 would increase the chance that Cd-metal will form.

e. Temperature

The effects of temperature on stability could not be predicted because of insufficient kinetic data.

2.2.2 Comparisons Between Electron and Reactor Radiations

From the standpoint of potentially available radiation intensities and relative simplicity of experiments, it was evident that the use of fast electrons from an available Van de Graaff accelerator would be preferable to in-pile experiments. In assessing the probable significance of results of Van

---

*It is assumed that about 50 percent of e^-_{aq} should react with H^+ in order to cause an appreciable effect.

de Graaff experiments, use was made of the results of calculations of the type mentioned above.[1] Assuming as before that the only reactions of the Cd-ions are No. 33 and 25, Table 2, the calculated concentration of Cd^{+1} does not change appreciably with radiation intensity, and the concentrations under electron irradiation are slightly greater than those in the reactor ar the same intensity.* If oxidizing reactions of Cd^{+1} with H_2O_2 are, in fact, important, we would expect the difference to be still greater since the concentrations of these oxidizing species are greatest for reactor radiations.[1] Accordingly, it was concluded that electron irradiation could provide a severe test of the effects of reactor operation on the solution stability.

2.2.3 Agitation During Irradiation

It can be plausibly assumed that the separation of any insoluble material from the bulk of solution would occur at solid surfaces. If this were the case, the mixing of solution and the film conditions at a surface would be important. However, theoretical considerations did not enable us to predict reliably whether agitation would have any effect on the solution stability or, in fact, the direction of an effect if one occurred. Two types of experiments, static and dynamic, were therefore proposed in order to assure that the radiation stability would be tested under conditions at least as severe as those in the reactor where essentially static conditions prevail in some regions and rapid flow prevails in other regions. In the dynamic experiment, the solution would be circulated to produce heat and mass transfer coefficients between solution and walls comparable to maximum values in the reactor.

2.2.4 Container Material

On the chance that the surface material might affect the rate of separation of insoluble material, the container material would be of Zircaloy-2 as in the reactor.

---

*This difference in the calculated concentrations of Cd^{+1} stems from the differences between the yields, for electron and reactor radiations, of each of the several radiolytic products of water.

3 Methods

3.1 General

In the static experiments, small volumes (~15λ)* of a $CdSO_4$ solution were contained in Zircaloy-2 at a controlled (± 5°C) temperature in the range 60 to 120°C and were irradiated with electrons at power densities up to 150 w per cc of solution. After continuous irradiation for several min (usually 30 min), the solution was displaced with fresh solution so that the sample was forced thru a fine titanium filter** into a region outside of irradiation where it was collected for analysis of Cd. The displacement solution which was in the cell at the time irradiation was stopped (and the temperature reduced to 30 to 40°C) was also analyzed for Cd in most experiments. The effects of irradiation on solution stability were evaluated from comparisons between the results of these Cd analyses and those for control experiments without irradiation. The dose rate within the solution during an irradiation was determined from measurements of the electron current along with the previously determined relationship between current and power density for the experimental arrangement. The Zircaloy-2 container was a 0.066 cm ID, 0.10 cm OD tube bent into a loop of 1.3 cm diameter. The temperature of this tube was controlled by passage of controlled temperature water over the outer surface. The decision to use the very small bore tube resulted, primarily, from considerations of temperature gradients within the solution. At 150 w per cc the calculated gradient was 7.4°C, and this was thought to be near the maximum which we would tolerate.

The planned dynamic experiment was to be conducted with a small, high speed (35,000 rpm), centrifugal pump with which solution was to be circulated thru a small bore tube forming a loop in front of the cover plate of the pump.

---

* 1 λ = 0.001 ml.

** 3-3.5 μ pore size.

The diameters of the pump cavity and of the tube bore were about one-half inch and 26 mils, respectively. The total fluid volume was about one-fourth cc, and all of the fluid was to be irradiated continuously during exposure. The purpose of the tube was to provide a channel in which film conditions could be made comparable to those in the reactor. The flow around the impeller and housing could not be well defined, so the film conditions in this region could not be estimated reliably. The selection of the bore diameter was based on: (1) calculated values for the solution velocity required in a tube of given bore diameter to establish film coefficients comparable to those in the reactor at a velocity and hydraulic diameter of 40 fps and 100 mils, (2) experimental values for head-flow characteristics of a pump which was designed and tested, and (3) experimental values for the flow rate-pressure drop relationship in a 26 mil ID tube bent into the shape required with the cell. The effects of irradiation on solution stability in this system were also to be evaluated from comparisons between results of analyses for Cd in irradiated and control solutions.

3.2 Evaluations of Electron Dose Rate and Uniformity

The ORNL Chemistry Division Van de Graaff Accelerator which was used in this work could deliver a maximum, continuous, electron current of 100 μamps at 2 Mev. Electron energies of 1.95 to 2 Mev were used in all experiments.

Before designing the cells, measurements were made of beam uniformity and intensity as a function of target size and location and of the presence of beam scatterers in front of a target. The results were used to estimate the maximum diameter of a cell in which the solution could be uniformly irradiated at 150 w per cc. The thicknesses of the target solution and of the container materials for which electron energy would be deposited in the solution at the maximum, uniform rate were evaluated from considerations of the known depth-dose characteristics of an electron beam. Following these measurements and considerations, static and dynamic cell mock-ups were employed in dose rate measurements using a ceric sulfate dosimeter solution. Relationships between total electron current and average dose rate to the solution were determined for the static system in these measurements. The results of these measurements provided additional bases for the selection of cell dimensions. Thus, the diameter and thickness of solution and container for the proposed pumped system was near the maximum for which approximately uniform power densities of 150 w per cc of solution could be produced. The diameter of the static loop was also near the maximum for approximately uniform power densities of 150 w per cc of solution.

This work is described in more detail in Section 4.

3.3 Sorption of Cadmium on Surfaces Out-of-Radiation

A few measurements were made of the sorption of cadmium on Zircaloy-2, stainless steel, and titanium in order to estimate the acceptability of a material or of a surface preparation for use in our experiments.

These tests were carried out by placing the metal surface in contact with a test solution at a temperature of interest and for a period of time in excess of 30 min. Following exposure, the surface was rinsed with water and then with 0.05 M HNO_3. The HNO_3 rinse was collected for analysis of cadmium.

3.4 Miscellaneous

Measurements were made of the pH of two irradiated samples in search of confirmatory evidence of degree of solution stability.

The static loop used in the final experiments was dismantled, examined, and the surfaces were leached with 2 M HCl after rinsing with water. The acid solutions were analyzed for Cd.

4. Evaluations of Electron Dose Rate and Uniformity

4.1 Uniformity of Dose Across Thickness of Cell

Methods and information employed in considerations of this factor are detailed in Appendix I. The dimensions of both the static and proposed dynamic cells were chosen to be such that the rate of loss of electron beam energy to the solution was near the maximum and was approximately uniform across the cell.

4.2 Beam Uniformity and Dependence Upon Scatterers and Position at Van de Graaff

Preliminary measurements of the electron beam intensity and uniformity were made using a collector plate mounted behind (30 mil separation) a cylindrical hole in a shield plate. The two plates were electrically insulated. The thickness of each plate (1/4 in. brass or copper) was sufficient to absorb all impinging electrons.

The results are plotted in Fig. II-1, Appendix II. They showed that a current sufficient for an average power density of 150 w per cc could be obtained within a cell which is 1.35 cm or less in diameter. However, the current density over the surface of the cell was far from uniform, and the extent of nonuniformity was outside the limits considered suitable (± 25%) for the stability experiments.

Considerations of methods of producing a more nearly uniform current density indicated that metal foils between the beam and the target might produce the desired effect and these were tried.

Equipment for measurements of the effects of beam scatterer was comprised of thirteen, 62-mil, copper pins mounted in holes drilled in a 1/4 in. brass plate. The pins were mounted flush with the front surface of the plate and were electrically insulated by a 4 mil radial air gap for part of the thickness of the plate (front 1/8 in.) and by an 8 mil Micarta sleeve for the remainder. The pins were located on concentric circles of 0.277, 0.437 and 0.595 cm radii. Four pins were on each of these circles and one was at the center. The scatterers were centrally positioned and held by two narrow strips of the scattering material (Fig. 6).

The conditions tested and the results are recorded in Appendix III.

The results showed that scatterers are effective in producing a more nearly uniform beam over the areas of interest. Typically, the current density near the center was reduced while that at the outer edge was increased. On the basis of these results it was expected that a power density of 150 w per cc could be readily achieved in a static cell using a 1.3 cm loop. The results also showed that an approximately uniform beam could be obtained over the larger surface areas required with the dynamic cell (1.3 cm diameter). The average current density in this case would produce a power density of about 115 w per cc if the electrons made only one pass through the solution. However, there was reason to expect that the additional passes caused by backscattering would increase the power density to 150 w per cc.

4.3 Dosimetry Measurements in Mock-ups of Static and Dynamic Cells

The experiments which employed the ceric sulfate dosimeter solution are described in detail in Appendix IV.

The tests with the static cell mock-up showed that a power density of 145 w per cc of water could be produced at 100 μamps total current in a cell with dimensions as listed in Table 3 and with scatterer and spatial arrangements as follows: Gold scatterer, 0.6 cm diameter and 1 mil thick, located 0.48 cm from plane of test loop. Distance between planes of loop and Van de Graaff window; 2.27 cm. Shield plate in front of loop; 0.32 cm thick brass with 1.27 diameter central hole. Inner surface of plate 0.16 cm from plane of test loop. The results also established the relationship between power density and total electron current between 50 and 100 μamps. On the basis of results of pin measurements (Sec. 4.2), the maximum variation in power density was ± 7% for this arrangement.

The results of the dosimetry experiments with the dynamic cell mock-ups indicated that a fairly uniform power density of about 150 w per cc at 100 μamps could be achieved in the proposed dynamic cell. The existence of a nearly uniform power density was deduced from results reported in Section 4.2 for the uniformity of current density for the cell and scatterer positions used (Exp. 8 of Appendix III, 2.91 cm window separation with 1 mil Au separated from the cell by 0.48 cm). Since the thickness of the window and of the solution in an experimental cell would differ from those in the mock-up, the relationship between current and power density for the experimental cell was not necessarily well established. It is believed that additional dosimetry experiments in which the ceric solution would be exposed within the cell would be required for this purpose.

It is interesting to note that back-scattering of electrons into the solutions (also side scattering with the static mock-up) contributed importantly to the power density in both dynamic and static mock-ups. Power densities of about 93 and 107 w per cc of water at 100 μamps were predicted for the static and dynamic mock-ups in the absence of scattering. The experimental power densities were 145 ± 12 and 153 ± 23 w per cc water, respectively. These errors for the 70% confidence limit were evaluated from the scatter of the experimental data for $G(Ce^{+3})$ as well as that for production of Ce^{+3} during electron irradiations.

5 Equipment for Static Experiments

5.1 Assembly

The experimental assembly was comprised, primarily, of (1) the cell in which solution was irradiated at a controlled temperature, (2) auxiliary equipment for the introduction of solution samples into the cell and for their recovery, and (3) equipment for preheating tap water to a controlled temperature before passage of the water thru the cell jacket. A schematic drawing showing components and interconnections of the solution system is given in Fig. 1. A photograph of the assembled equipment is shown in Fig. 2. The cell is behind the drift tube of the electron accelerator and, thus, does not appear.

5.2 Cell

5.2.1 Dimensions

A photograph of the cell and jacket is shown in Fig. 3 and a drawing of the irradiation assembly is given in Fig. 4. Nominal dimensions are listed in the latter figure. The ID and length of the Zircaloy-2 tubing differed slightly from one cell to another, and the actual dimensions are listed in Table 3.

The OD was 40 mils in each case.

The pore size of the titanium filter was 0.0003 to 0.00035 cm. The diameter was that of the enlarged end of the Zircaloy-2 tube (Table 3). The thickness was 30 mils.

5.2.2 Joint Connections

Joint connections between the Zircaloy-2 and stainless steel cooling jacket were accomplished as described in Fig. 4. Those between Zircaloy-2 and the 6-mil stainless steel tubing were made as described in Fig. 4 only in the case of cell No. 4. For cells 1 and 2, these connections were made as shown in Fig. 5. The combination of connections and mounting arrangement (see below) used with cell No. 4 proved to be the most reliable.

5.2.3 Zircaloy-2 Material

Zircaloy-2 capillary tubing which had been obtained several years ago from a commercial source was used in fabrication of the cell.* The internal and external diameters of the as-received tubing were 22.5 and 40 mils. Before use, the internal surface of the tubing was chemically polished (50 cc H_2O, 50 cc conc. HNO_3, and 10 cc 48% HF) to produce a surface which had a satisfactory appearance and upon which adsorption of Cd was apparently negligible (see below). The ID was enlarged to 26 mils in this process.

5.2.4 Fabrication of Cell and Jacket

The detailed procedure for fabrication of the test loop is given in Appendix V.

---

*We had planned to use tubing fabricated at ORNL by machining and drawing. However, leaks were found in each of several test pieces after they were formed into loops, and the material was, accordingly, judged unsatisfactory.

Table 3. Dimensions and Volumes of Experimental Static Cells

Component	Parameter	Cell No. 1[a]	Cell No. 2[b]	Cell No. 4[c]
Irradiated portion of Zircaloy-2	Length (cm)	4.4	4.1	4.1
	I.D. (cm)	0.066	0.064	0.066
	Volume cc	0.015	0.013	0.014
	Volume (steps on piston)	245	141	152
	Surface Area (cm^2)	0.92	0.82	0.85
Zircaloy-2 between filter and stainless tubing	Length (cm)	1.9	2.2	2.1
	I.D. (cm)	0.071	0.075	0.071
	Volume (cc)	0.0076	0.0098	0.0084
	Volume (steps on piston)	121	107	91
Stainless steel tubing between cell and collection chamber	Length (cm)	20	20	20
	I.D. (cm)	0.016	0.016	0.016
	Volume (cc)	0.0042	0.0042	0.0042
	Volume (steps on piston)	68	46	46

[a] Piston stem No. 1

[b] Piston stem No. 2

[c] Piston stem Nos. 2 and 3.

5.2.5 Cell-mounting Arrangement

Brass plates and other equipment used to support a cell during irradiation are illustrated in Fig. 4. Dimensions and descriptive material for most of this equipment are included in the figure. The cell was attached to the large plate in such a way that the cell and all coolant water lines were thermally insulated from the plate. A photograph of the mounting equipment as seen from the front surface of the Van de Graaff drift tube is shown in Fig. 6. The gold foil used to scatter the electron beam is at the center of the assembly. Part of the cell can be seen thru the opening in the second plate.

Details of the cell-4 attachment to the large plate are illustrated in Fig. 7 and referenced features are described below.

(a) The stainless steel tubing was clamped firmly to a metal block. The Zircaloy-2 tubing was attached and sealed to the stainless by means of a small amount of epoxy cement but it was not clamped directly.

(b) Metal blocks placed as indicated were used to shield the epoxy joints between (a) and (b) from scattered electron irradiation and to act as a support and as a guide in which the Zircaloy-2 tubing could move to reliable thermal stresses.

(c) Metal hoods shielded the epoxy joints on the jacket connector from scattered electron irradiation.

(d) Each of the coolant water lines was clamped at two points with thermal insulation between the lines and the plate. These points were located away from the loop so that the lines would flex readily as the cell moved in response to changes in temperature. The two-point mounting precluded stressing of the cell upon movement of the external water lines.

5.2.6 Location at Van de Graaff

The spatial arrangements at the Van de Graaff coincided with those used in dosimetry measurements (Sec. 4.3). The scatterer material and dimensions were also the same.

5.2.7 Temperature Gradients in Cell

As stated above, the temperature of the cell was controlled by passage of controlled-temperature water thru the jacket. During irradiation, the heat generated within the solution and test tube caused their temperatures to rise above that of the coolant. Also, the temperature of the coolant increased while in the cell. Estimates of these temperature gradients for cells 1 and 4 (Table 3) at 150 w per cc of solution are set forth in Table 4. The values which were used for heating rates within cell components are listed in Table 5. Values for flow rates, Reynolds' numbers, and fluid film coefficients are listed in Table 6. The estimated temperature gradients for cell-2 differed only slightly from those listed because of the slight differences between internal diameters of cell-2 and of cells 1 and 4 (Table 3).

The estimated temperature differences between coolant and inner surface of Zircaloy-2 ranged from about 2.4 to 3.3°C (Table 4). The temperature at the center of the solution was 7.3°C above the wall.

5.3 Reservoir

The reservoir (Figs. 1 and 2) was made from a titanium cylinder, 1.5 in. ID and 24.5 in. in depth. A drawing of the reservoir has been published.[22]

Table 4. Calculated Temperature Gradients in Static Test Loop (150 w/cc)

Location	Temperature Gradient at 60°C	Temperature Gradient at 77 and 120°C[e]
1. Portion of Zircaloy-2 containing solution	(°C)	(°C)
Center of solution to inner surface of tube	7.3[a]	7.3[a]
Across Zircaloy-2 wall		
Volume heating in wall	.78[b]	.78[b]
Heat from solution	0.25[b]	0.25[b]
Total	1.0	1.0
Across film between Zircaloy-2 and coolant		
Turbulent flow	-	1.4 (h = 13,100)[f]
Transition flow	2.2 (h = 8,600)[c]	-
Total from inner Zircaloy-2 surface to coolant	3.3	2.4
Total from center of solution to coolant	10.5	9.7
2. Portion of tube containing titanium filter		
Center of titanium to inner surface of tube	1.1[d] (minimum)	1.1[d] (minimum)
Across Zircaloy-2 wall	0.9[b] (maximum	0.9[b] (maxium)
Across film between Zircaloy-2 and coolant		
Turbulent flow	-	1.3 (h = 13,100)[f]
Transition flow	1.9 (h = 8,600)[c]	-
Total from inner Zircaloy-2 surface to coolant	2.8	2.2
Total from center of filter to coolant	4.0	3.3
3. Temperature rise in coolant at 3.80 cc/sec (19 fps)	0.62/cm	0.62/cm

a,b,c,d, Methods of calculation described in Appendixes of Ref. 22 as follows:

- a. Appendix 1.
- b. Appendix 2.
- c. Appendix 3. See text and Table 6 in this report.
- d. Appendix 4.
- e. It was assumed that the values of all parameters were the same as those at 60°C except those influencing the film coefficient.
- f. See Table 6 and text. Calculated values ranged from 13,100 to 15,300. Acordingly, some of the temperature gradients across the film were slightly less than these values.

Table 5. Calculated Radiation Heating in Components of Reference Static Test Loop at 150 w/cc in Solution

Component	Heating Rate	
1. Test sample tube	$(\text{cal}, \text{sec}^{-1}, \text{cm}^{-1})^{a,b}$	$(\text{cal}, \text{sec}^{-1}, \text{cm}^{-2})^{c}$
Solution	0.13	0.41
Zircaloy-2 wall	0.75	2.34
Total of solution plus wall	0.88	2.75
2. Coolant jacket		
Water	0.25	--
Stainless steel	1.22	--
3. Total heat flowing into water (neglecting filter)	2.35	--
4. Titanium filter	0.44[d]	2.4[e]

[a] Per unit length of loop.

[b] Relative heating rate per unit volume. Water-39, Zr-156, stainless steel-226, Ti-130 (Ref. 22, p. 5).

[c] Per unit area of outer surface of Zircaloy-2 tubing.

[d] For a density of 3.8 g/cc.

[e] For filter plus Zircaloy-2 wall.

Table 6. Flow Rates Thru Cell-Jackets, Calculated Reynolds' Numbers and Calculated Film Coefficient on Outer Surface of Zircaloy-2 Tube

Cell No.	Temperature (°C)	Flow Rate (cc/sec)[a]	(fps)[b]	Re[b]	h (Btu/hr/ft^2/F)
1	60	3.63	18	4,200	8,600[c]
1	120	3.00-3.33	15-17	7,100-7,900	13,100-14,000[d]
1R	120	3.75	19	8,900	15,300[d]
2	60	3.93	20	4,600	8,600[c]
2	120	3.26	16	7,700	13,600[d]
4	77	4.42	22	6,600	14,400[d]

a. Observed

b. Calculated

c. Calculated for 19 fps, Re = 4,400 and transition zone flow. (Ref.22 Appendix 3). Approximately the same values obtained for the listed values of Re and velocity.

d. Calculated for fully developed turbulent flow as previously reported. (Ref.22, Appendix 3).

5.4 Displacement Piston

The displacement piston (Figs. 1 and 2) was comprised of a titanium valve with Teflon packing manufactured by Autoclave Engineers, Erie, Pa. (30,000 psi series). This was operated removely using a step-motor.

Three different valve stems were used during experiments. Stems 1 and 3 were of titanium while stem-2 was of stainless steel.

The relationship between movement of one step on the motor and volume displacement was determined using a 20 λ pipet attached to the discharge side of the piston. This relationship for stem-1 was 6.25×10^{-5} cc/step. For stems 2 and 3 it was 9.19×10^{-5} cc/step.

5.5 Sample Collection Chamber

A drawing of this chamber showing materials and dimensions is given in Fig. 8. Provisions for control of He pressure and for adding wash-solution under pressure are illustrated in Fig. 1. A special feature was the provision for detecting liquid at the tip of the tube which joined the chamber and the cell (Fig. 8, Section BB). The electrode was constructed of a 20 mil platinum wire sealed within but insulated from a 60 mil OD platinum tube using glass to effect the seal and insulation. The spacing between the electrode and the tip was adjusted with the aid of a screw arrangement on the tube. The electrode could be positioned so that one step (6 to 9×10^{-5} cc) insertion or retraction of the piston made or broke the contact. Normally, the electrode was positioned so that one or two steps made or broke the contact.

Pressure seals at the electrode, tube, and cap were made using Teflon.

5.6 Valves and Connecting Tubing

Referring to Fig. 1, all connecting lines between the piston and the sample collection chamber were of 304 stainless steel capillary, 6 mil ID and 60 mil OD. The approximate lengths from the piston to connector to cell were 29 and 50 cm, respectively. That from the cell to the tip within the collection chamber was 20 cm. In the final assemblies, V-1 and P were connected with a 4.5 cm length of high pressure stainless steel tubing (1/4 in. OD, 80 mil ID), and the reservoir was joined to V-1 with a 3.5 cm length of 1/4 in. titanium tubing (Fig. 2). For some of the earlier experiments, the length of stainless steel tubing between V-1 and P was somewhat greater while the diameter was less than in the final assembly. Valve V-1 (Figs. 1 and 2) was of titanium (High Pressure Products). The second tube at the bottom of the reservoir (Fig. 2) was capped using a stainless steel fitting.

5.7 Coolant Temperature Control

The initial system for control of coolant temperature employed a 1500 w heater (ref. 22, Fig. 6) controlled by a Variac. Filtered tap water under supply pressure (60 psig) passed through the heater and coolant jacket in sequence. The jacket discharge pressure was 0 psig for operating temperatures below 100°C, and 15 to 20 psig for temperatures above 100°C. The higher discharge pressure was obtained by means of a flow restrictor. In practice this system proved satisfactory at an operating temperature of 60°C. However, an operating temperature of 120°C could not be achieved because of boiling on the heater surfaces and consequent flow reductions.

The following modifications of the heating system were made to overcome this difficulty: (1) A second 1500 w heater was installed in series with the first, (2) a 250 w tape heater was wrapped around the one-eighth inch copper tube which conducted water from the 1500 w heaters into the jacket of the cell, and (3) hot (~60°C) tap water was used as the feed-water supply. The second 1500 w heater was of the same design as the first, and the power in this heater was also controlled thru a Variac. For operation at 120°C, the power in each of these heaters was a fraction of full power. The tape heater was operated at full voltage. Temperature control with this system was adequate when the flow rate was about 180 cc per min or greater. However, it also failed at lower flow rates because of boiling in the 1500 w heaters.

The 1500 w heaters were electrically insulated from the cell and frame using a length of Teflon tube on the discharge side of the heaters.* The water lines within the heaters were then grounded.

5.8 Performance of Equipment

The components and assembly could be made to operate satisfactorily, and successful experiments were conducted with results reported in Sec. 8. However, difficulties were encountered which delayed experimentation. Major ones are described below.

a. Leaks in cell assembly

Leaks occurred at the epoxy joints on several occasions. These resulted from thermal and mechanical stresses and from radiation damage to the cement. The mounting and shielding arrangements used with cell-4 were designed to minimize these factors and were eminently satisfactory.

---

*Insulation of cell and frame from ground was necessary for measurement of beam currents.

Two cells developed leaks across the Zircaloy-2 wall between the solution and jacket regions. In each case, these leaks occurred shortly after the cell was put into use. In one case, cell-3, the leak occurred before any experiments could be completed. The ID of the Zircaloy-2 was oversize in these cases, and it is believed that the leaks resulted from defects in the metal which were uncovered by excessive removal of metal during polishing.

b. Piston

The Teflon stem-packing on the piston developed leaks on several occasions. These caused difficulties in removing gas bubbles from the solution as well as causing loss of solution during pressurization. The gas bubbles were presumably introduced thru the leak when the piston was evacuated as part of the usual procedure followed in freeing the system of gas.

The stainless steel stem could not be used with a pH 2 solution because of an apparent reaction with this solution. However, it was unaffected in the neutral salt solutions.

Stalling of the step-motor caused by binding of the piston-drive arrangement was encountered on several occasions.

c. Stability of $CdSO_4$ solutions within equipment

On one occasion, the analytical results of experiments (Appendix VI) showed variations between the concentrations of Cd which led us to believe that Cd-bearing solids were deposited at some locations and that more or less of this solid was redissolved by the solution which was passed during flushing operations. In order to remove any such deposits, the entire system was flushed with 0.08 M HNO_3.

Following this acid flush, severe difficulties were encountered in freeing the solution system of gas, and there were indications that gas was generated within the reservoir; presumably from a reaction between the titanium and the solution. In an attempt to passivate any active surfaces, the titanium reservoir was exposed to 5% HNO_3 at 90°C for about one hr. Following this, the gas-bubble content of the system could be reduced to an acceptable level.

6 Test of Sorption of Cd Out-of-Radiation

6.1 Zircaloy-2 Tubes

Information on the amount of Cd sorbed on the Zircaloy-2 tube in the static system in the absence of radiation was needed for the design of radiation experiments and for the interpretation of results. Several preliminary sorption experiments were carried out using Zircaloy-2 tubing prepared in our shops and having dimensions near those in the experimental systems. Sorption on the internal surface was tested.

A sorption test was carried out by placing the surface in contact with the test solution for 30 min. One cc of water was then passed through the tube to rinse out the test solution. One-tenth cc of 0.01 M HNO_3 was then passed thru the tube and collected for analyses. The HNO_3 solution contacted the surface for about 10 min.

A list of exposure temperatures and of results of analyses is set forth in Table 7. The solution was 0.04 M $CdSO_4$. Sulfuric acid at 0.01 M was added for a few experiments as noted.

Test piece No. 1 was 4.8 cm long, 0.11 cm OD, 0.052 cm ID, 0.77 cm^2 internal area and 0.0103 cc internal volume. This tube was used in the as-received

Table 7. Results of Analyses for Cd in Tests of Sorption on Zircaloy-2

Experiment Number	Test Piece Number	Exposure Temperature (°C)	Cd in Sample (μg total)	Cd in Sample ($\mu g/cm^2$)
1	1	room	2.3	3.0
2	1	90	3.3	4.3
3	1	90	4.1	5.3
4[a]	1	120	3.6	4.7
5	1	90	< 0.5	-
6	1	90	2.7	3.5
7[b]	1	90	0.9	1.2
8[b]	1	90	< 0.5	-
13[c]	1	90	7.9	10.3
14	2	room	3.4	3.4
15	2	90	< 0.5	-
16	2	90	< 0.5	-

a. Test piece and solution sealed in glass and placed in 120°C oven for 1.5 hr. Exposure time for other experiments was 30 min.

b. 0.01 M H_2SO_4 in test solution.

c. Tube exposed to 300°C steam for 1 hr prior to test.

condition in consecutive experiments 1 thru 4. Prior to Exp. 5 the surface was contacted with 0.01 M HNO_3 at room temperature for 1 hr and was then used in consecutive Exps. 5 thru 8. The tube surface then was contacted with 8 M HNO_3 at room temperature for 1.5 hr and a steam-oxygen mixture (15 psi) at 300°C for 1 hr, and then used in Exp. 13. The tube was rinsed with water prior to each experiment.

Test piece No. 2 was 5.0 cm long, 0.112 cm OD, 0.066 cm ID, 1.0 cm^2 internal area and 0.017 cc internal volume. The internal surface was abraded and chemically polished (50 cc H_2O, 50 cc conc. HNO_3, 10 cc 48% HF) prior to use. About 6 mils on the diameter were removed in this polishing to give the final 0.066 cm ID. This tube was used in Exps. 14 thru 16.

Microscopic examination of surface No. 1 revealed that dark oxide was present initially. After the 300°C steam treatment white oxide was also present. The surface of No. 2 had a metallic luster with no apparent oxide.

The results were insufficient to draw definite conclusions. They indicated that sorption occurred on the oxide and that the amount sorbed changed with the amount of oxide. Thus the greatest amount of sorption was found in Exp. 13 for which the amount of oxide was also greatest. Also, reduction of the amount of oxide by chemical polishing (Exps. 14-16) effected a reduction of the amount sorbed in two of the experiments (compare Exps. 1-4 with 14-16).

Since it was considered desirable to have minimum out-of-radiation sorption on the Zircaloy-2 test loops, these loops were chemically polished prior to use. The results of two sorption experiments on each of two test loops using the above procedures showed that an undetectable amount of Cd was sorbed on the polished surfaces at room temperature, $< 0.13\ \mu g/cm^2$. Also, the results of control experiments conducted during the radiation experiments (Sec.11) did not reveal any increase in sorption at elevated temperatures.

6.2 Stainless Steel Capillary, Type 304.

One experiment was made to test sorption of Cd on the 6 mil ID stainless steel capillary which was employed in the test system. The method was similar to that described above. Exposures were made in 0.04 M $CdSO_4$ at room temperature. The analytical results showed $<0.5\ \mu g$ Cd per cm^2.

6.3 Titanium Filter Material

Tests were made on titanium filter material specimens the superficial areas of which were 1.0 cm^2. The procedures were similar to those described above but were modified so that test and rinse solutions were forced thru the filter. The results of two tests each at room temperature and at 90°C were 3.5 and 5.5 $\mu g\ Cd/cm^2$ and 9.8 and 15.8 $\mu g\ Cd/cm^2$. Since the superficial area of the filter used in a radiation experiment was about 0.008 cm^2, the total sorption was expected to be $< 0.1\ \mu g$ at the maximum. This amount was considered negligible.

6.4 Brazing Alloy

Tests were made of the corrosion resistance and cadmium sorption of the brazing alloy proposed for use with the dynamic cell.* Test pieces (~ 3 cm^2) were exposed overnight in 0.04 M $CdSO_4$ at 90°C. No change in weight was

---

*ORNL brazing alloy RGG 7 (titanium 48%, zirconium 48%, beryllium 4%).

observed, and the Cd sorption was below detection limits, $< 0.2\ \mu g/cm^2$.

7 Procedure for Stability Experiments

7.1 Experiments Employing Solution Analyses

7.1.1 Final Experiments

As stated in Section 3, about 15 λ of solution were irradiated during an experiment. Quantitative sampling of this small volume was accomplished by expelling the solution into the collection chamber where it formed a droplet on the tip of the stainless steel tube. The chamber was depressurized, opened, and a 10 λ sample withdrawn using a calibrated pipet. Procedures for control samples duplicated those of the irradiation samples so that any evaporative changes of concentration within the droplet prior to sampling were also duplicated.

Two other sampling procedures were tried during preliminary experimentation but were unsatisfactory because of poor reproducibility. In both of these a droplet of known volume was to be formed by moving the piston a known amount, and this known volume was to be recovered quantitatively for analyses. In one procedure, the sample was washed from the tip into the bottom of the collection chamber while the chamber was still pressurized with He. In the other, the chamber was depressurized and opened before washing the droplet from the tip. Attempts to develop these procedures were abandoned when it was found that good reproducibility could be achieved by pipeting directly from the droplet.

The step by step procedure adopted is given below.

Refer to Fig. 1 for identification of the components of system.

1. Charge reservoir with $CdSO_4$ solution and pressurize with He to 450 psi.
2. Disconnect the line leading to cell at connector, F, and pass 0.05 M HNO_3

solution thru the cell entering in S. Acid is in contact with cell for 5 min.[a]

3. Re-make connection and fill lines between R and S with reservoir solution in such a way that all air is displaced.

4. Pass reservoir solution into S until the pH of solution entering S is the same as that in R.

5. Clean S, and cover wide part of bottom with 0.05 M HNO_3 or water.

6. Pressurize S with He (60 to 350 psi)[b].

7. Measure compressibility by inserting P until contact on probe.

8. Measure leak rate (leak rates ranged between 0 and 3 steps per min).

9. Insert P until contact on probe and then retract piston 15 to 25 steps.

10. Raise cell temperature to experimental temperature from that of cold tap water.

11. Insert P until contact on probe and then retract to bring the level near the filter in cell.

12. Measure leak rate.

13. Hold for 30 min with irradiation (or without irradiation for control tests) and then insert P to form a droplet on the tip of the probe containing at least 13 λ of solution.

14. Shut off Van de Graaff.

15. Shut off power to heaters.

16. Depressurize S by venting thru V-4 after cell temperature is below about 37°C.

---

a. In early experiments, a tee connection leading to a valve was used in place of the connector. The acid flush solution was introduced at the tee. Some of the early experiments also differed in other, minor, details.

b. Pressurization was needed to suppress boiling of the test solution, to keep gases in solution, and to achieve close coupling between movement of the piston and the liquid-gas interface.

17. Open S and pipet 10 λ from the approximately 13 to 15 λ droplet.

18. Clean S, repressurize and measure compressibility.

19. Open S and insert P to displace most of the solution which was in the line between the filter and the probe at the time irradiation was terminated. Discard this solution.

20. Clean S and cover the wide portion of the bottom with 0.05 M HNO_3.

21. Insert P to form a sample droplet comprised mainly of the solution which was in the cell when irradiation was terminated.

22. Remove 10 λ sample from droplet.

23. Repeat steps for additional experiments.

A solution of 1 M HCl was used in transferring analytical samples from the pipet into a 10 ml volumetric flask. The analyst diluted the sample to 10 ml and determined Cd^{+2} concentration polarographically.

The procedures for the control experiments were the same as those listed except that the Van de Graaff was not operated.

Samples of the reservoir solution were collected at intervals during a series of experiments. For these, the solution was passed rapidly into S after the flushing operation prior to an experiment was completed. A portion of the solution was placed in a flask and, for the most of the experiments, 10 λ samples were withdrawn for analyses at a later time.

Usually, three control and three irradiation experiments were made at a given set of test conditions in order to improve and establish the precision of results. Fewer experiments were made in some cases because of shortage of time available for experimentation. An irradiation experiment and a control for comparison were made within a period of a few hr except for the experiments reported in Table 8. In this set of experiments,which were the first of the final experiments, some of the controls and radiation tests were made on different days.

A significant change in sampling procedure was made following completion of the experiments in Table 8. Initially, a sample was pipeted from the droplet by one worker who watched both the droplet and the level within the pipet. Overfilling and underfilling of the pipet occurred, with consequent possible loss of precision. In the revised, satisfactory, procedure one worker watched the level in the pipet while the other watched the droplet and operated the pipet.

7.1.2 Initial Experiments (Tables 18 and 19)

The initial experiments employed exposure times of 5 and 50 min rather than 30 min. The procedures were basically the same as those described above for the experiments in Table 8. However, they were less refined in several respects; (1) It is possible that procedure step 5 in which dilute acid or water was placed on the bottom of the collection chamber was omitted in some of these experiments. This omission would favor vaporization from a sample droplet and, consequently, a high result; (2) Valve V-6, Fig. 1, was leaky so that an uncontrolled amount of dry He passed over a sample droplet during the time of sample withdrawal in the case of A-type samples and during droplet formation and sample withdrawal for the B-type samples; and (3) Control and radiation experiments were conducted on different days.

7.2 Experiments Employing pH Measurements

Two experiments were made in which the sample was analyzed for pH. Twenty λ samples were required so that the sample droplet ($\sim$22 λ) contained some solution which had not been irradiated for 30 min. Other procedure steps were essentially the same as those above. Water was placed in S during an experiment. No exact control experiments were made although experiments of a control type were performed. In these, a droplet was formed on the probe while the cell was at low temperature just prior to irradiation. The droplet was sampled and analyzed for pH.

8 Results of Stability Experiments Employing Solution Analyses

8.1 Final Experiments

8.1.1 Tabulations of Results

The results of stability experiments at several different sets of conditions are listed in Tables 8 and 9 and 11-14. The irradiated and irradiation-control samples are designated as A-samples. The follow-up samples of the solution which was in the cell when irradiation was stopped and the temperature was reduced (or just the temperature reduced with control samples) are designated as B-samples. Differences between cadmium concentrations in sets of control and radiation samples are included in all tables except 8. Values for the average of the differences and of the calculated standard errors of the averages are also listed. Most of the data in Table 8 could not be separated into comparative sets, and, accordingly, the averages of the analytical values are listed.

The data in Table 9 indicated a shift in concentration levels for samples obtained and analyzed on different days. Some reanalyses of reservoir solutions from these and previous experiments were carried out in search of an explanation for this shift. The results, presented in Table 10, showed that the actual concentration levels in the reservoir solutions did not change significantly. Considerations of this and of the nature of the analyses led us to believe that the shift resulted from a change in the calibration of the polarograph on 4/6/66. Some of the smaller shifts in concentration levels observed with other test conditions may have the same explanation, e.g., Table 11.*

Table 15 contains a summary of the averages of concentration differences between radiation and control samples. Calculated values for standard errors and for errors at the 80% confidence limit are also listed. Additional error calculations were made in which it was assumed the results obtained with 0.02 M $CdSO_4$ solutions at 100 μamps and at both 77 and 120°C could be treated as though they were exposed under the same conditions. In further error analyses, the results obtained with 0.02 M $CdSO_4$ at 75 μamps were also included. A summary of the results of these additional error analyses is given in Table 16.

Table 17 shows values for the average of differences between A- and B-type control samples (that is, of differences between samples obtained in a given experiment) and the results of error analyses for these values.

8.1.2 Discussion of Treatment of Data

The exposure and sampling procedures and conditions for the A-type control samples were essentially the same, except for the absence of radiation, as those for A-type radiation samples. Accordingly, any systematic effects on Cd concentrations in a radiation sample, for example, vaporization from or con-

---

*An error in calibration of the polarograph would not appreciably affect differences between radiation and control samples which were analyzed using the given calibration since the same error existed for each sample.

densation into the sample droplet, were balanced by those in the accompanying control experiment. Significant differences between concentrations can, therefore, be ascribed to effects of irradiation. Similarly, the B-type control and radiation samples were essentially the same except for the presence or absence of radiations during the exposure of the preceding A-sample and during the few min required to displace the A-sample. Again, any significant difference in Cd concentration between a set of radiation and control samples can be ascribed to an effect of irradiation.

As stated above, the reported errors for gain or loss of cadmium shown by A- and B-samples were based, where possible, on consideration of the difference between sets of radiation and control experiments. With this approach, scatter resulting from replenishment or replacement of the reservoir solution with fresh stock or from day to day shifts in reported concentration levels were not included in the calculated error.

The reported standard errors were calculated using the equation,

$$\text{S.E.} = \pm \sqrt{\Sigma(x - \bar{x})^2/n(n-1)},$$

where $x - \bar{x}$ is the difference between an experimental value and the average value, and n is the number of data points. The confidence limits were calculated by multiplying the standard error by the t-value appropriate to the number of data points and to the percentage confidence limit of interest.

The procedures for collecting A- and B-type samples differed with respect to the conditions maintained during droplet formation. The droplet for an A-type sample was formed while the collection chamber was pressurized with He. That for the B-type was formed while the chamber contained air at atmospheric pressure. In other respects, however, the procedures and conditions were comparable. In the case of the control experiments, comparisons between results of the A- and B-samples (Table 17) provide information on the combined effects of elevated temperatures on Cd sorption and of the maintenance of different pressure conditions during droplet formation. They also provide information on the reproducibility of sampling and analyses.

The true concentrations of Cd in the reservoir solution were not necessarily the same as those in the droplet at the time of sampling even though no change in concentration occurred during passage from the reservoir to the droplet. This is because some evaporation from or condensation into the droplet may have taken place while it was in the chamber. Also, the reproducibility of the reservoir samples was not necessarily representative of those of A or B samples since the sampling procedures differed. Specifically, with the reservoir samples a small volume of solution was placed in a 10 ml volumetric flask from which 10 λ samples were withdrawn at a later time. The outside of the pipet may have been contaminated with Cd over an appreciable length when it was inserted into a flask, and failure to remove all traces of contamination before transfer of the 10 λ sample into the final sample flask would have affected the results. Also, sorption on the glass flask from the high pH solutions may have affected the concentration. For the A and B samples, the outside of the pipet was contaminated only over a very short length near the tip, and, hence, the chances were very small that this contamination was not quantitatively removed during washing prior to transferring the sample into the sample flask. In effect, then, the results of analyses of reservoir solutions were used only to detect appreciable changes in the concentration of the reservoir solution and/or changes in the calibration of the analytical equipment.

8.2 Initial Experiments

The data for these experiments are listed in Tables 18 and 19. The designations employed for samples of a given type are the same as those described above. The data were not separated into comparative sets because they were either too few or the scatter was too great to justify this approach.

For the 5 min exposures, the difference between the average amounts of Cd in the A-type control and radiation samples was 1.2 μg ± 2.0 μg standard error. Thus, within the standard error (± 3%) no loss of Cd resulting from irradiation was detected. The few data obtained with the B-type samples did not contribute any additional information.

The 50 min-exposure data were too few and too scattered to permit fruitful comparisons between results of control and irradiation experiments.

With respect to the possible occurrence of a difference between the amounts of Cd lost during 5- and 50-min exposures, it can be seen that the difference between the averages of A-type radiation samples for the two times was 2.2 μg while the standard errors were ± 0.5 and ± 0.6 μg. The concentrations of Cd in the reservoir solutions did not differ significantly for the different-time experiments so that, prior to irradiation, the concentration of Cd in the A-type samples presumably did not differ either. Accordingly, if it is further presumed that the concentration differences did not result from random differences in experimental procedures (Sec. 7.1.2), these data indicate that Cd loss was greatest at the longer time.

9 Results and Discussion of Stability Experiments Employing pH Measurements

The results of the pH measurements are listed in Table 20. The pH values of the irradiated samples were definitely less than those of the initial solution and of the control* experiments.

It can be assumed that the reductions in pH resulted from the formation of reduced species (for example Cd^{o}), and estimates were made of the amounts of reduced species required to produce the observed pH values. The results of such estimates depend strongly upon assumptions regarding the effective concentrations of $SO_4^{=}$ in the solution. This is because of the equilibrium,

$$HSO_4^- \rightleftarrows SO_4^{=} + H^+, \ K = 0.0103 \text{ at } 25°C.$$

If it is assumed that the effective concentration of $SO_4^{=}$ is approximately that of $CdSO_4$, the observed reductions in pH would be explained by reduction of 0.8 to 1.5% of the Cd^{+2} to Cd^{o}. However, the results of our measurements of the pH of 0.067 M $CdSO_4$ solutions to which small amounts of H_2SO_4 were added indicated that only a small part (~10%) of the $CdSO_4$ was taking part in the above reaction. If this were the case in fact, then the reductions in pH could be accounted for by reduction of 0.2 to 0.3% of the Cd^{+2}.

It was concluded that these measurements indicated that a reduction of $CdSO_4$ occurred and that the fraction reduced was 0.2 to 1.5% of the amount initially present.

10 Results of Examination of Cell-4

Visual examination of the Zircaloy-2 test tube revealed that the interior

---

*As mentioned previously the controls were held in the cell at low temperature for a short period of time.

surfaces were clean and bright as expected for chemically polished surfaces. There were no apparent differences between surfaces exposed and unexposed to radiation.

No cadmium was detected in the 2M HCl solutions used to leach the filter and sections of the unexposed and exposed tubing. Each surface was flushed with water prior to leaching. Time of contact with the acid leach was 10 min for the Zircaloy-2 sections and 3 min for the titanium filter. The acid was not forced thru the filter during the leach. The Zircaloy-2 surface areas and limits of Cd detection corresponded to limits of Cd detection per unit area of $< 0.2\ \mu g/cm^2$ for the irradiated portion of the tube (3.5 cm length) and $< 0.3\ \mu g/cm^2$ on the unirradiated portion (2.4 cm length from the inlet side).

11 Discussion of Results of Stability Experiments

11.1 A and B Control Samples

a. Stability of solutions out-of-radiation

The results of averaging and error analyses set forth in Table 17 show that for 0.02 M $CdSO_4$ control experiments the concentrations of Cd in A and B samples were the same within the detection limits. The small average differences are less than the standard errors. Results at 77 and 120°C are indistinguishable. If significant amounts of Cd had been lost by sorption from the A-samples at elevated temperatures, either an equivalent amount was lost from the follow-up samples during the short time they were at high temperature, or the loss must have been closely compensated by vaporization which caused the A-droplet to be concentrated, relative to the B-droplet, by the proper amount.* Both alternatives were considered very unlikely, and it was concluded

---

*As stated previously, sorption at room temperature was expected to be below detection limits; $< 0.13\ \mu g/cm^2$.

that Cd sorption out-of-radiation was probably below detection limits of about 0.5 μg/cm^2 at both 77 and 120°C.

Similar considerations of the control data from final experiments with 0.067 M $CdSO_4$ (Table 17) led to similar conclusions.

b. Precision of data

Comparisons between error values listed in Table 17 and those for A-type control and radiation samples listed in Tables 15 and 16 show near agreement, in most cases, between comparable groups of data. For example, in Table 17 the standard errors for data from Tables 9, 11, 12 and 13 are, respectively, ± 0.6, 1.7, 1.3 and 2.2%. For A-sample data in Table 15, the standard errors are ± 0.5, 1.1, 1.5 and 1.4%. The comparable error values for B-sample data in Table 16 are somewhat greater; ± 1.3, 1.9, 0.7 and 2.7%. The results of these comparisons show that the variation of the difference between control and radiation type samples reflect random errors in sampling of the same nature as those for the control data in Table 17.

11.2 Loss of Cadmium During Experimental Irradiations

The A-sample data for the final experiments (Table 15) show small losses of cadmium during irradiation for each set of experimental conditions. The indicated occurrence of a loss is significant at the 80% confidence level for data reported in Tables 9, 11 and 12 and at about the 70% level for Table 13 data. The small loss indicated by the average of data in Table 8 cannot be considered significant. The difference between the loss in 0.02 M $CdSO_4$ at 120°C and 100 μamps (Table 11) and that in 0.02 M $CdSO_4$ at 77°C and 50 μamps (Table 13) is significant at the 70% level. The smaller differences between other sets of conditions are not significant (significant only at level of 50% or less).

Since each of the several groups of data from final experiments show loss of Cd, the overall confidence that Cd was lost during irradiation is greater than that shown by results of error analysis of an individual group. This is demonstrated by the error analyses shown in Table 16. Here, the combined experimental values from Tables 11 and 12 and from Tables 11, 12 and 13 show losses of Cd in excess of 95% confidence limits.

Our general conclusions from the final experiments are that Cd was lost from the solutions during irradiation at all test conditions. The fractions lost from a solution of given concentration was probably greater at 120° than at 77 or 60°C. The fraction lost from 0.02 M solution was probably less at 50 μamp than at the higher radiation intensity, and it was probably less at pH 2 than at the pH of the neutral salt.

The actual amounts lost under experimental conditions of Tables 9-13 are probably represented best by the percentage values listed in column 5 of Table 15. The value of 4.5% loss for the experimental conditions of Table 8 (0.067 M, 120°C, 100 μamps) is thought to be the best indication of behavior under these conditions.

The results of preliminary experiments indicated that the amount of Cd lost during irradiation depended upon exposure time for the conditions tested (0.067 M $CdSO_4$, 60°C, 100 μamps for 5 and 50 min).

11.3 Recovery of Cadmium in Follow-up Samples (B-Samples)

The B-sample results (Table 15) indicated that the solution which displaced the radiation sample was enriched in Cd at a majority of the experimental conditions. However, the enrichments were less than the losses of Cd from the radiation samples, and the standard errors for the enrichments were generally greater. Consequently, with one exception, the indications of enrichment are not significant. The indication of enrichment by the data in Table 11 is significant at about the 70% level. The combined data of Tables 11 and 12 (Table 16) show the occurrence of enrichment at the 80% confidence limit.

The general conclusion is that the majority of the Cd lost during irradiation did not redissolve during the period between stopping of irradiation and expulsion of the follow-up sample.* Presumably, it was dissolved during the HNO_3 acid flush which preceded each experiment.

11.4 Speculations Regarding Mechanism of Observed Radiation Effects and of Radiation Effects in the TWMR

The results of these experiments showed that electron irradiation of 0.067 and 0.02 M $CdSO_4$ solutions (pH of the neutral salt) produces loss of cadmium from the solutions. The data indicated that only small fractions of the separated material are readily soluble in the $CdSO_4$ solutions. They also indicated that the amount of Cd lost increases with irradiation time. These results together with theoretical considerations discussed in Sec. 2.2 suggest a picture of radiolysis described by Eqs. a-c.

$$\frac{d(Cd_s^o)}{dt} = K_f - K_s(Cd_s^o) - K_w(Cd_s^o) \qquad \text{(a)}$$

$$\frac{d(Cd_s^o)}{dt} = K_w(Cd_s^o) - K_w^1(Cd_w^o) \qquad \text{(b)}$$

---

*Mixing of fresh solution with the sample during displacement did not occur to the extent necessary to explain the low Cd recovery. This was shown in an experiment in which a dyed solution was used to displace water within a glass mock-up of the cell (without filter). The diffuse front of the dyed solution was always near the position calculated from the piston displacement, and this indicated that mixing and channeling were negligible.

$$\frac{d(Cd^{+2})}{dt} = - K_f + K_s(Cd_s^o) + K_w^1(Cd_w^o) \qquad (c)$$

In these equations, Cd_s^o is the material which separates from the solution. This material dissolves to reform Cd^{+2} (Eq. (c)) but it also changes into a form, Cd_w^o, which is less soluble (Eq. (b)). This change might consist of agglomeration into larger particles or of deposition on solid surfaces. The rate of formation of Cd_s^o is represented by K_f, and from theoretical considerations this rate is probably constant after a few sec irradiation if the solution composition remains approximately constant.

It can be seen that for certain selected values of K_f, K_s and K_w, K_w^1, the concentrations of Cd_s^o would be low and approximately constant while that of Cd^{+2} continued to decrease thru formation of relatively insoluble Cd_w^o. Accordingly, the loss of Cd might be negligible during short exposures but appreciable during longer ones.

Assuming that this picture of radiolysis of $CdSO_4$ solutions in the experiments is valid, we expect that the same solutions will suffer more, less, or the same degree of solid formation in the TWMR at comparable radiation times depending upon the values of K_f, K_s, K_w and K_w^1 relative to those in this experimental work. While K_f would probably be somewhat lower in reactor irradiations (Sec. 2.2.2) and the kinetic behavior would be affected to some extent by circulation of solution outside the core, the largest difference in behavior may result from effects of agitation and from differences between surface area to volume ratios. Agitation of solution in the reactor would probably affect the rate of agglomeration or of deposition on a surface, K_w, and also the rate of dissolution of this material, K_w^1. If deposition of separated material on surfaces is important, the relatively low surface area to volume ratio in the reactor may affect the stability behavior relative to that in the experiments; again thru effects on K_w and K_w^1.

Additional experimental work designed to determine effects of agitation and of surface area to volume ratio on radiation stability would be required to more closely predict actual behavior.

12 Status of Dynamic System

The design of the dynamic experiment along with results of component testing for the design have been reported.[22] Some additional experimental work was done to establish the feasibility of constructing the end cap with tubing brazed in place. This was reported in the Monthly Report for April.[23] Detailed design drawings were also included in this monthly report.

Table 8

Results of Tests of Stability of 0.06 7 M $CdSO_4$ at 120°C and 100 μamps

(150 w/cc)

(Cell 1)

Date	Sample No.[a]	Amount of Cd in 10λ of Solution (μg)				
		Control		Radiation		Reservoir[d]
		A[b]	B[c]	A[b]	B[c]	
3/9	146-147	60.9	60.3	-	-	-
	148	-	-	-	-	59.6
	149	-	-	-	-	59.4
	150-151	-	-	58.2	61.7	-
3/11	151A	-	-	-	-	59.3
	152	-	-	-	-	59.1
	153-154	54.6[e]	61.6	-	-	-
3/13	154A-155	-	63.6	-	-	-
	156	-	-	-	-	59.0
	157	-	-	-	-	60.2
	159-160	60.0	60.2	-	-	-
	161	-	-	-	-	62.4
	162	-	-	-	-	61.9
	163	58.6	-	-	-	-
3/15	165-166	-	-	59.4	59.8	-
	168	-	-	-	-	60.8
	171	-	-	61.1	-	-
	171A	-	-	-	-	61.8
Average		59.8	61.4	59.5	60.8	60.1
Standard error of average		±0.7	±0.8	±0.8	±0.9	± 0.4

---

a. Exposure time for radiation and control experiments was 30 min.

b. Sample of irradiated or control solution.

c. Sample of solution in cell at time irradiation or control was terminated.

d. Sample of reservoir solution collected in S and then placed in flask from which 10λ samples were withdrawn at a later time.

e. Sample No. 153 was omitted from the average. A statistical basis exists for this omission.

Table 9

Results of Tests of Stability of 0.067 M $CdSO_4$ at 60° and 100 μamps

(150 w/cc)

(Cell 2)

Date	Sample No.[a]	Amount of Cd in 10λ of Solution (μg) Control A[b]	Control B[c]	Radiation A[b]	Radiation B[c]	Reservoir[d]	Radiation Values Less Control Values A (μg/10λ)	B (μg/10λ)
4/5	179-180	59.4	59.6	-	-	-	- 0.7	2.0
	181-182	-	-	58.7	61.6	-		
	183A	-	-	-	-	61.3		
	183B	-	-	-	-	60.7		
	184A	-	-	-	-	60.3		
4/6	185-186	56.3	55.3	-	-	-		
	188A	-	-	-	-	55.4	- 1.5	0.1
	188B					56.8		
	189-190	-	-	54.8	55.4	-		
	191-192	-	-	56.2	55.5	-		
	194A	-	-	-	-	57.3	- 0.4	- 0.7
	194B	-	-	-	-	56.7		
	195-196	56.6	56.2	-	-	-		
						Average	- 0.87	0.47
							± 0.33 SE	±.80 SE

---

a. Exposure time for control and radiation experiments was 30 min.

b. Sample of irradiated or control solution.

c. Sample of solution in cell at time irradiation or control was terminated.

d. Sample of reservoir solution collected in S and then placed in flask from which 10λ samples were withdrawn at a later time.

Table 10

Results of Initial Analyses and Reanalyses of Reservoir Solutions

Sample No. and Date[a]		Initial Analysis		Reanalysis[b,f]	
		Sample No.[f]	[Cd] (μg/10λ)	Sample No.	[Cd] (μg/10λ)
168[c]	3/15	168	60.8	168-5	63.2
				168-6	63.3
171A[c]	3/15	171A	61.8	-	-
187[d]	4/6	-	-	187-1	62.5
				187-2	61.2
188[d]	4/6	188A	55.4	188-7	69.6
		188-B	56.8	188-8	61.4
193[e]	4/6	-	-	193-1	61.1
				193-2	62.3
194[e]	4/6	194A	57.3	-	-
		194B	56.7	-	-

a. Large sample collected in 10 ml flask.

b. All samples analyzed on 4/21/66

c. Samples 168 and 171A were taken, respectively, prior to and following radiation experiment 171. They are considered to be duplicates.

d. Samples 187 and 188 were duplicates.

e. Samples 193 and 194 were duplicates.

f. 10λ sample taken from large sample.

Table 11. Results of Tests of Stability of 0.02 M $CdSO_4$ at 120°C and 100 µamps (150 w/cc)

Date	Cell No.	Sample No.[a]	Amount of Cd in 10λ of Solution (µg)					Radiation Values Less Control Values	
			Control		Radiation		Reservoir[d]	A (µg/10λ)	B (µg/10λ)
			A[b]	B[c]	A[b]	B[c]			
4/7	2	197-198	17.3	17.5	--	--	--	- 1.1	1.0
		199-200	--	--	16.2	18.5	--		
		201A	--	--	--	--	19.2		
		201B	--	--	--	--	16.8		
		201C	--	--	--	--	16.9		
4/26	1	206-207	19.1	18.7	--	--	--	- 0.7	0.3
		208-1	--	--	--	--	19.1		
		208-2	--	--	--	--	19.2		
		209-210	--	--	18.4	19.0	--		
		211-1	--	--	--	--	19.8		
		211-2	--	--	--	--	19.0		
							Av.	- 0.9 ± 0.2 SE	0.6 ± 0.4 SE

a. Exposure time for control and irradiation experiments was 30 min.

b. Sample of irradiated or control solution.

c. Sample of solution in cell at time irradiation or control was terminated.

d. Sample of reservoir solution collected in S and then placed in flask from which 10λ samples were withdrawn at a later time.

Table 12. Results of Tests of Stability of 0.02 M $CdSO_4$ at 77°C and 100 μamps (150 w/cc) (Cell 4)

Date	Sample No.[a]	Amount of Cd in 10λ of Solution (μg)					Radiation Values Less Control Values	
		Control		Radiation		Reservoir[d]		
		A[b]	B[c]	A[b]	B[c]		A (μg/10λ)	B (μg/10λ)
5/4	212-213	17.9	17.9	--	--	--		
	214-1	--	--	--	--	17.7	- 1.1	0
	214-2	--	--	--	--	17.8		
	215-216	--	--	16.8	17.9			
5/5	217-218	17.7	17.9	--	--	--		
	220-1	--	--	--	--	17.7	- 0.2	0
	220-2	--	--	--	--	17.5		
	221-222	--	--	17.5	17.9	--		
	223-224	--	--	18.0	18.3	--		
	226-1	--	--	--	--	18.3	- 0.5	0.4
	226-2	--	--	--	--	17.7		
	227-228	18.5	17.9	--	--	--		
						Av.	- 0.6	0.1
							± 0.3 SE	± 0.1 SE

a. Exposure time for control and radiation experiments was 30 min.

b. Sample of irradiated or control solution.

c. Sample of solution in cell at time irradiation or control was terminated.

d. Sample of reservoir solution collected in S and then placed in flask from which 10λ samples were withdrawn at a later time.

Table 13. Results of Tests of Stability of 0.02 M $CdSO_4$ at 77°C and 50 μamps (75 w/cc) (Cell 4)

Date	Sample No.[a]	Amount of Cd in 10λ of Solution (μg): Control A[b]	Control B[c]	Radiation A[b]	Radiation B[c]	Reservoir[d]	Radiation Values Less Control Values: A (μg/10λ)	B (μg/10λ)
5/11	250-1	--	--	--	--	18.1	- 0.4	0.2
	250-2	--	--	--	--	17.8		
	251-252	18.7	18.3	--	--	--		
	253-1	--	--	--	--	18.2		
	253-2	--	--	--	--	18.4		
	254-255	--	--	18.3	18.5	--		
5/23	258-1	--	--	--	--	17.6	- 0.8	- 1.4
	258-2	--	--	--	--	18.0		
	259-260	17.6	18.6	--	--			
	261-1	--	--	--	--	17.6		
	261-2	--	--	--	--	17.6		
	262-263	--	--	16.8	17.2	--		
5/25	267-1	--	--	--	--	17.6	+ 0.1	0
	267-2	--	--	--	--	17.5		
	268-269	17.6	17.8	--	--			
	270-1	--	--	--	--	17.5		
	270-2	--	--	--	--	17.6		
	271-272	--	--	17.7	17.8	--		
						Av.	- 0.4	- 0.4
							± 0.3 SE	± 0.5 SE

a. Exposure time for control and radiation experiments was 30 min.

b. Sample of irradiated or control solution.

c. Sample of solution in cell at time irradiation or control was terminated.

d. Sample of reservoir solution collected in S and then placed in flask from which 10λ samples were withdrawn at a later time.

Table 14. Results of Tests of Stability of 0.02 M $CdSO_4$, pH-2, at 77°C and 100 μamps (75 w/cc) (Cell 4)

Date	Sample No.[a]	Amount of Cd in 10λ of Solution (μg)					Radiation Values Less Control Values	
		Control		Radiation		Reservoir[d]		
		A[b]	B[c]	A[b]	B[c]		A (μg/10λ)	B (μg/10λ)
5/31	285-1	--	--	--	--	17.8		
	285-2	--	--	--	--	17.8		
	286-287	17.8	17.6	--	--	--		
	288-1	--	--	--	--	17.6	- 0.2	0.8
	288-2	--	--	--	--	17.5		
	289-290	--	--	17.6	18.4	--		

a. Exposure time for control and radiation experiments was 30 min.

b. Sample of irradiated or control solution.

c. Sample of solution in cell at time irradiation or control was terminated.

d. Sample of reservoir solution collected in S and then placed in flask from which 10λ samples were withdrawn at a later time.

Table 15. Summary of Results of Stability Experiments Employing Analyses for Cadmium Concentrations

Reference Table No.	Concentration $CdSO_4$ (M)	Temperature[a] (°C)	Summary of A-Samples: Loss of Cadmium from Rad. Sample (μg/10λ)	(%)[b]	Standard Error (±μg/10λ)	(±%)[b]	Error at 80% Confidence (±μg/10λ)	(±%)[b]	Summary for B-Samples: Gain of Cadmium in Rad. Sample (μg/10λ)	(%)[b]	Standard Error (±μg/10λ)	(±%)[b]	Error at 80% Confidence (±μg/10λ)	(±%)[b]	Comments
8	0.067	120	0.3	0.5	1.1	1.8	1.7	2.8	- 0.6	- 1.0	1.3	2.2	2.0	3.4	c
8 Samples 146-147 150-151	0.067	120	2.7	4.5	-	-	-	-	1.4	2.3	-	-	-	-	d
9	0.067	60	0.9	1.5	0.3	0.5	0.6	1.0	0.5	0.8	0.8	1.3	1.5	2.5	
11	0.02	120	0.9	5.0	0.2	1.1	0.6	3.4	0.6	3.6	0.4	1.9	1.1	5.8	
12	0.02	77	0.6	3.3	0.3	1.5	0.5	2.8	0.1	0.7	0.1	0.7	0.2	1.3	
13	0.02	77	0.4	2.0	0.3	1.4	0.5	2.7	- 0.4	- 2.2	0.5	2.8	0.9	5.3	e
14	0.02[g]	77	0.2	1	-	-	-	-	0.8	4	-	-	-	-	f

a. Temperature of coolant water.

b. On the bases of 60 and 18 μg/10λ for 0.067 and 0.02 M solutions, respectively.

c. Error calculated for difference between averages of experimental values. Others calculated for average of difference between values in sets of radiation and control experiments.

d. This set of control and radiation experiments carried out under conditions for which direct comparisons were possible.

e. Bombardment current of 50 μamps (73 w/cc). Current for all other experiments was 100 μamps (145 w/cc).

f. One set of radiation and control experiments with this pH 2 solution.

g. pH 2 with H_2SO_4.

Table 16. Summary of Error for Combined Results of Experiments with Neutral 0.02 M $CdSO_4$

Reference Table No.	Sample Type	Loss of Cadmium in Radiation Samples		Standard Error		Error at 95% Confidence		Comments
		(μg/10λ)	(%)[c]	(±μg/10λ)	(± %)[c]	(±μg/10λ)	(± %)[c]	
11-12	A	0.72	4.0	0.17	1.0	0.47	2.7	a
	B	- 0.34	- 1.9	0.18	1.0	0.51	2.8	a
11-12-13	A	0.59	3.3	0.15	0.8	0.35	2.0	b
	B	- 0.06	- 0.3	0.24	1.3	0.57	3.1	b

a. All data for neutral 0.02 M $CdSO_4$ at 100 μamps.

b. All data for neutral 0.02 M $CdSO_4$ including 100 and 50 μamps irradiations.

c. On the basis of 18 μg per 10λ solution.

Table 17. Summary of Error for Difference Between A and B Control Samples

Reference Table No.	Concentration $CdSO_4$ (M)	Temperature (°C)	Average Amount of Cd in A Less that in B[a]		Standard Error		Error at 95% Confidence		Comments
			(μg/10 λ)	(±%)[b]	(±μg/10λ)	(±%)[b]	(±μg/10 λ)	(±%)[b]	
8	0.067	120	0.20	0.3	0.40	0.7	--	--	
9	0.067	60	0.40	0.7	0.38	0.6	--	--	
8-9	0.067	60-120	0.32	0.5	0.32	0.5	0.89	1.5	c
11	0.02	120	0.10	0.6	0.30	1.7	--	--	
12	0.02	77	0.13	0.7	0.24	1.3	--	--	
11-12	0.02	77-120	0.12	0.7	0.16	0.9	0.45	2.5	d
13	0.02	77	- 0.27	- 1.5	0.41	2.2	--	--	
11-12-13	0.02	77-120	- 0.10	- 0.6	0.17	1.0	0.41	2.3	e
12-13	0.02	77	- 0.20	- 1.1	0.21	1.2	0.54	3.1	
14	0.02 pH-2	77	0.20	1.1	--	--	--	--	f

a. All samples for which direct comparisons could be made.

b. On the basis of 60 and 18 μg per 10λ for 0.067 and 0.02 M solutions, respectively.

c. Data for 0.067 M $CdSO_4$ at 100 μamps and 60 and 120°C.

d. Data for neutral 0.02 M $CdSO_4$ at 100 μamps and 77 and 120°C.

e. Same as (d) plus data for neutral 0.02 M $CdSO_4$ at 75 μamps and 77°C.

f. One experiment.

Table 18

Results of Initial Tests of Stability of 0.067 M $CdSO_4$ at 60°C and 100 μamp (150 w/cc) for 5 min.

(Cell 1)

Date	Sample No.	Amount of Cd in 10λ of Solution (μg)				
		Control		Radiation		Reservoir[d]
		A[a]	B[b]	A[a]	B[b]	
2/18	114	67.7	-			
	115			63.5	-	
	116			62.0	-	
	117					8.19 mg/ml[c]
	118					8.17 mg/ml[c]
2/23	118A					61.7
	119					62.4
	120-121	61.1	63.8			
	122-123			63.6	66.3	
	124					61.8
	125					61.8
	126-127	63.8	62.6			
Average		64.2	63.2	63.0	-	61.9
Standard Error of Average		± 1.9	± 0.6	± 0.5	-	± 0.2

a. Sample of irradiated or control solution.

b. Sample of solution in cell at time irradiation or control was terminated.

c. A large volume of solution was submitted for analysis. We were not able to relate the results of these analyses to those for the 10λ samples. These results not included in average.

d. Sample of reservoir solution collected in S and then placed in flask from which 10λ samples were withdrawn at a later time.

Table 19

Results of Initial Tests of Stability of 0.067 M $CdSO_4$ at 60°C and 100 μamp (150 w/cc) for 50-min.

(Cell 1)

Date	Sample No.	Amount of Cd in 10λ of Solution (μg)				
		Control		Radiation		Reservoir[c]
		A[a]	B[b]	A[a]	B[b]	
2/25	130	67.5	-			
	131					62.3
	132					62.6
	133-134			61.3	67.2	
	135					62.6
	136					61.0
	137-138			60.3	63.4	62.1
Average		-	-	60.8	65.3	62.1
Standard error of average		-	-	± 0.6	± 1.9	± 0.4

a. Sample of irradiated or control solution.

b. Sample of solution in cell at time irradiation or control was terminated.

c. Sample of reservoir solution collected in S and then placed in flask from which 10λ samples were withdrawn at a later time.

Table 20. Results of pH Measurements on Irradiated Samples[a]

Sample No.[e]	Description of Sample	pH[b]
139-1	Control prior to irradiation	d
139-2	Control prior to irradiation	d
139-3	Irradiation sample	4.06
139-4	Solution in cell when irradiation was terminated	4.96
140-1	Control prior to irradiation	5.01
140-2	Control prior to irradiation	4.96
140-3	Irradiation sample	4.30
140-4	Solution in cell when irradiation was terminated	4.83

a. 0.067 M $CdSO_4$ irradiated for 10 min at 60°C.

b. pH of reservoir solution was 4.81.

c. Droplet size - 22λ.

d. No pH reading obtained.

e. Date of measurement, 3/1/66.

ORNL DWG. 66-2625

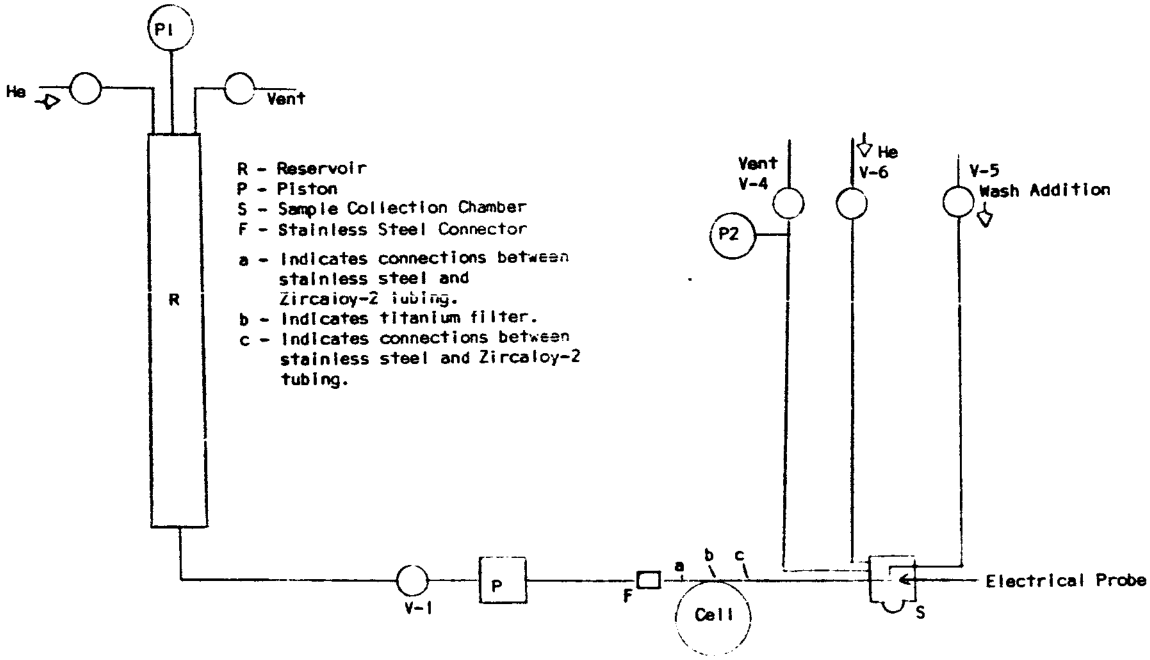

Fig. 1. Schematic of Static System

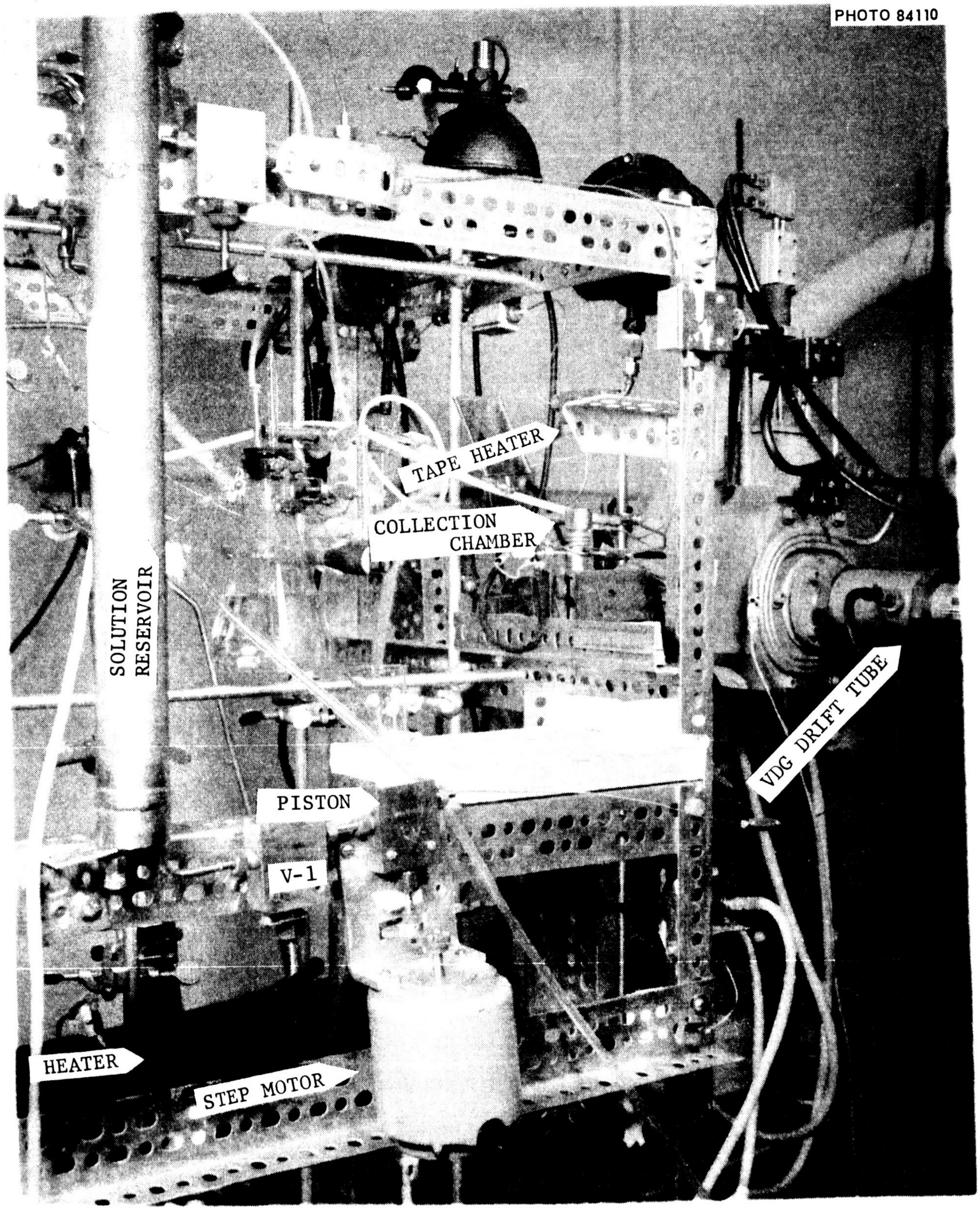

Fig. 2. Static Irradiation Assembly

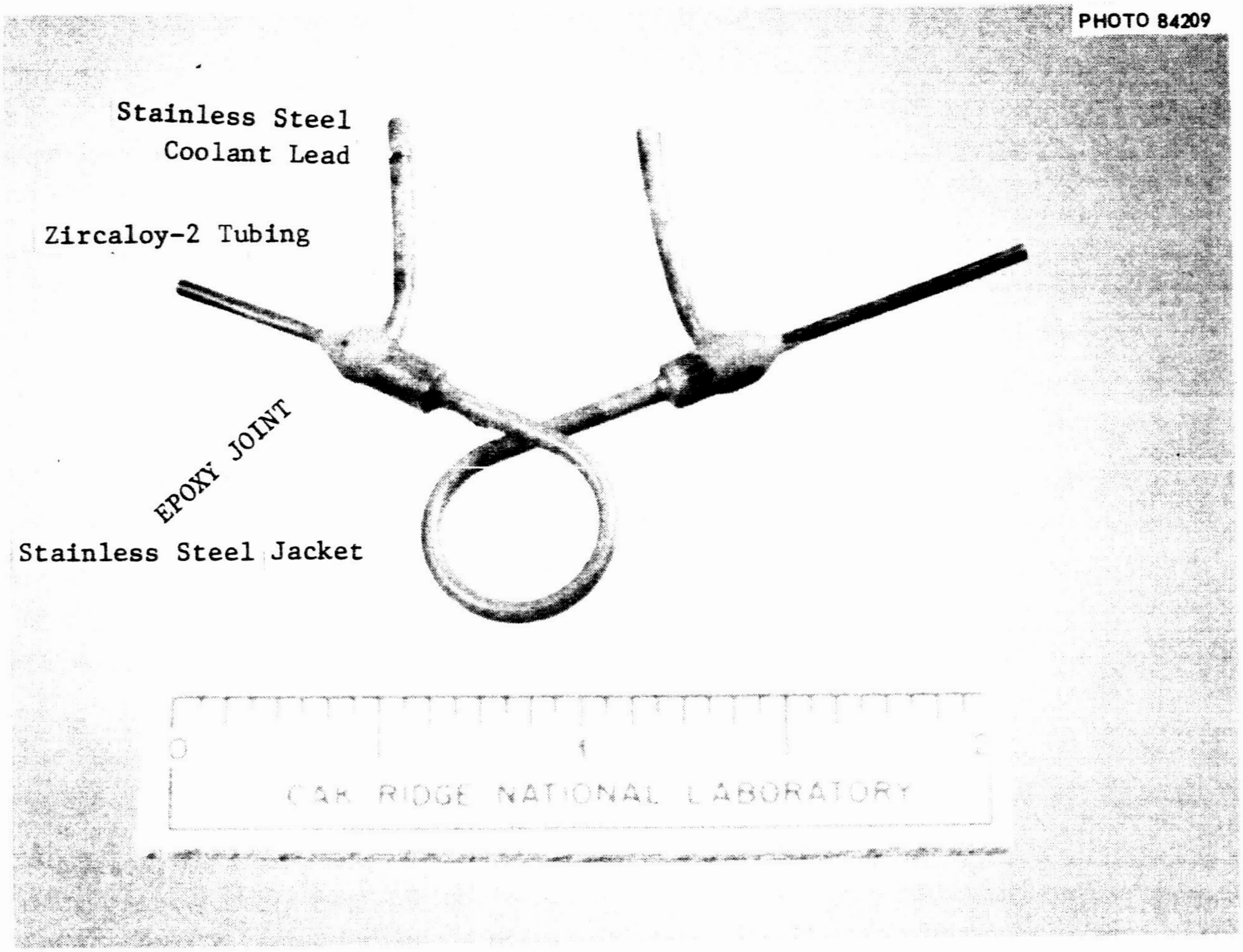

Fig. 3. Static Cell-Jacket Assembly.

Part No.	Part Name	Material	Dimensions and Descriptions
1	Test tube	Zircaloy-2	26 mil I.D.; 40 mil O.D. tubing. Coil diameter of 1/2-in. Length of irradiated portion, 1.6-in. Test tube is mounted such that poor thermal contact exists with mounting or shield plates.
2	Cooling jacket	Stainless Steel	62 mil O.D.; 54 mil I.D. tubing.
3	Solution inlet-outlet	Stainless Steel	6 mil I.D.; 60 mil O.D. Sealed to test tube with epoxy cement.
4	Shield plate	Brass	3-in. diam. x 1/8-in. thick spaced so that it clears test coil. Hole is 1/2-in. diam.
5	Controlled temperature water lines	Stainless Steel	62 mil O.D.; 54 mil I.D. tubing.
6	Clamp	Brass	5/8-in. x 5/8-in. x 1/4-in.
7	Clamp	Brass	5/8-in. x 5/8-in. x 1/4-in.
8	Water cooling tube	Copper	3/16-in. O.D.
9	Electron beam scatterer	Gold	1 mil thick, 1/4-in. diam. located 3/16-in. from plane of coil.
10	Water cooling tube	Copper	3/16-in. O.D.
11	Mounting Plate	Brass	4-1/2-in. diam x 1/4-in. thick.
12	Adapter	Stainless Steel	Joints between Zircaloy-2 and S.S. sealed with epoxy cement, others silver soldered.
13	Filter	Titanium	30 mil thick.

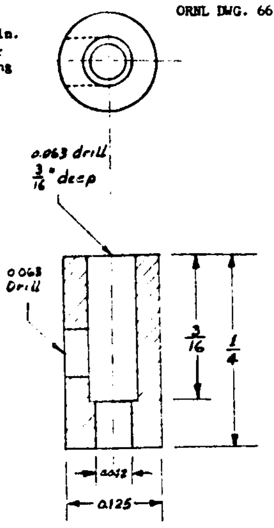

DETAIL ITEM (12)

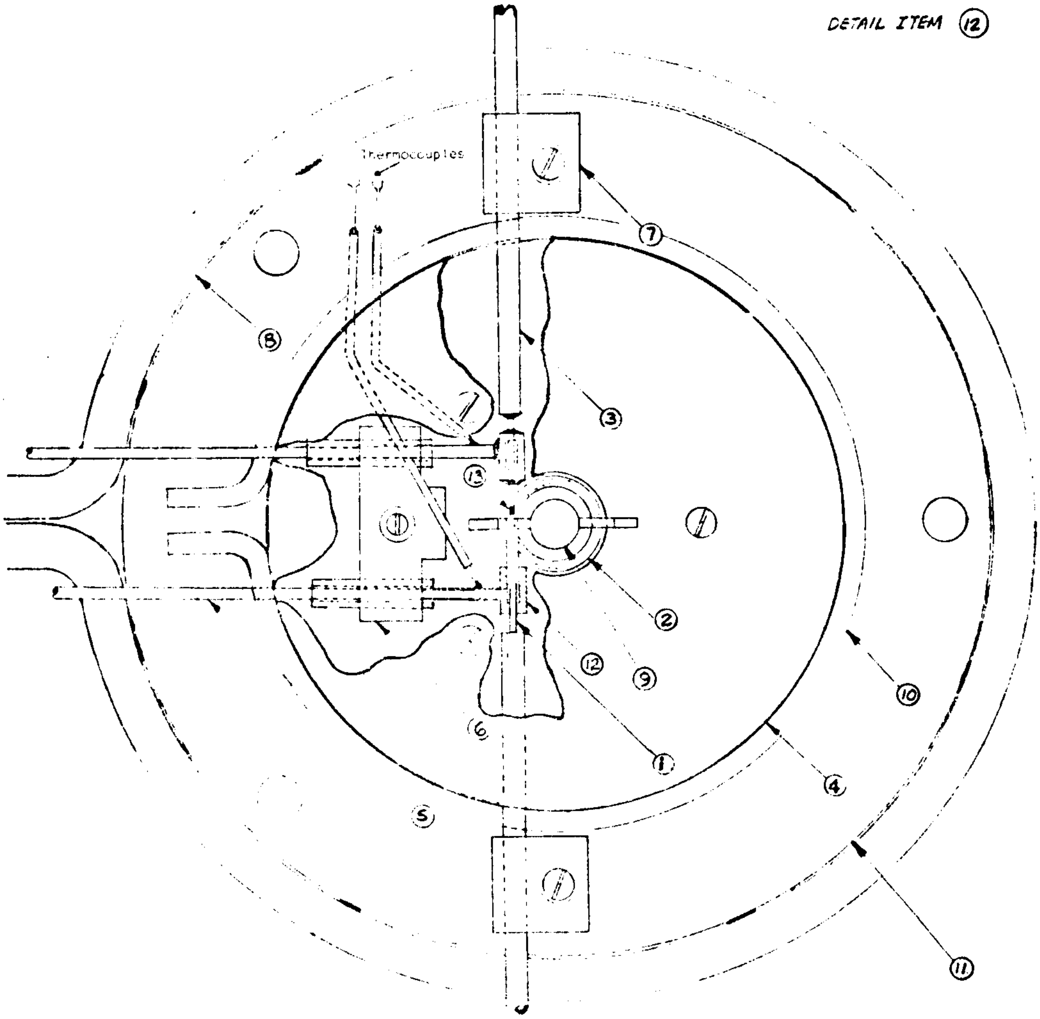

Fig. 4. Static Irradiation Cell.

ORNL DWG. 66-2626

A - 1"

B - 3/8" Hex.

C - 5/16" Hex.

D - 0.060" O.D. x 0.006 I.D.

E - 0.040" O.D. x 0.028 I.D.

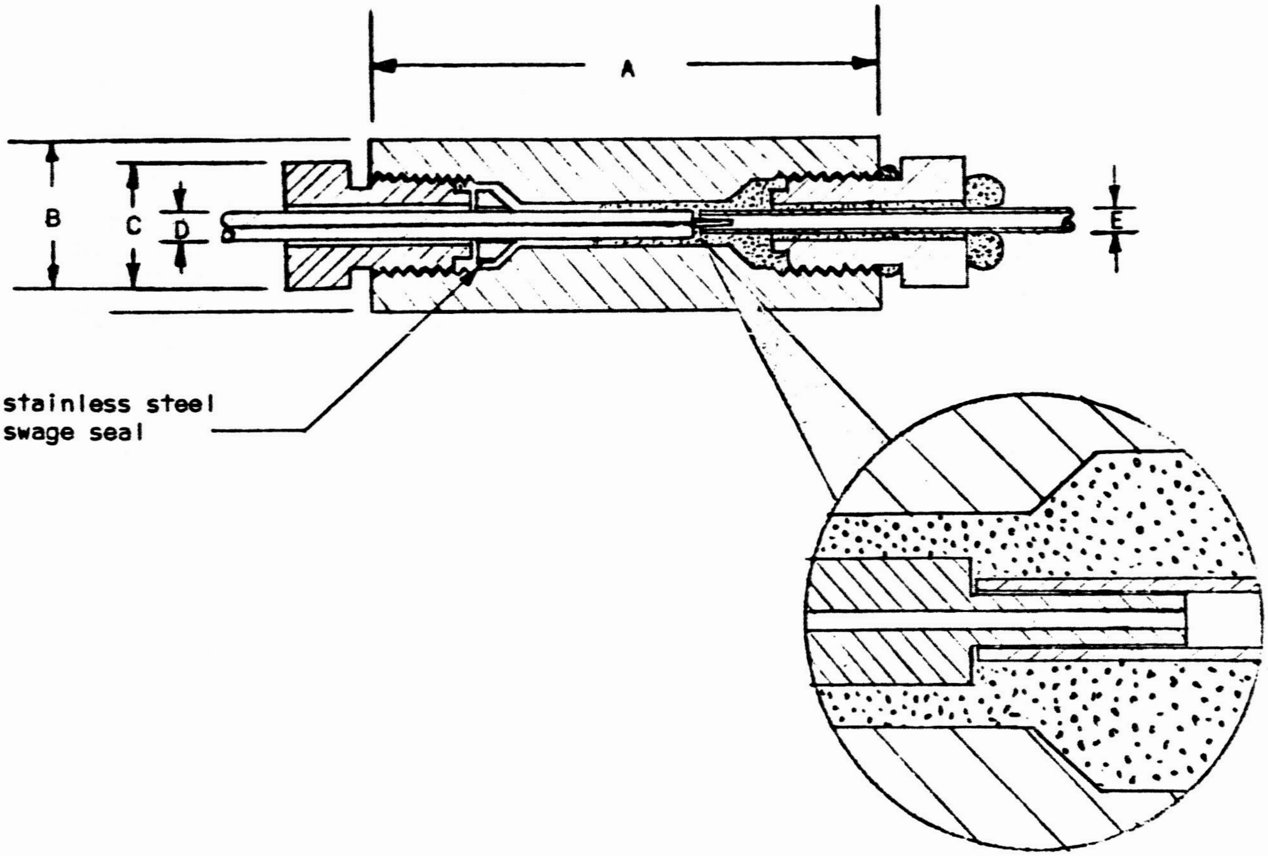

Fig. 5. Joint Between Zircaloy-2 and Stainless Steel Tubing.

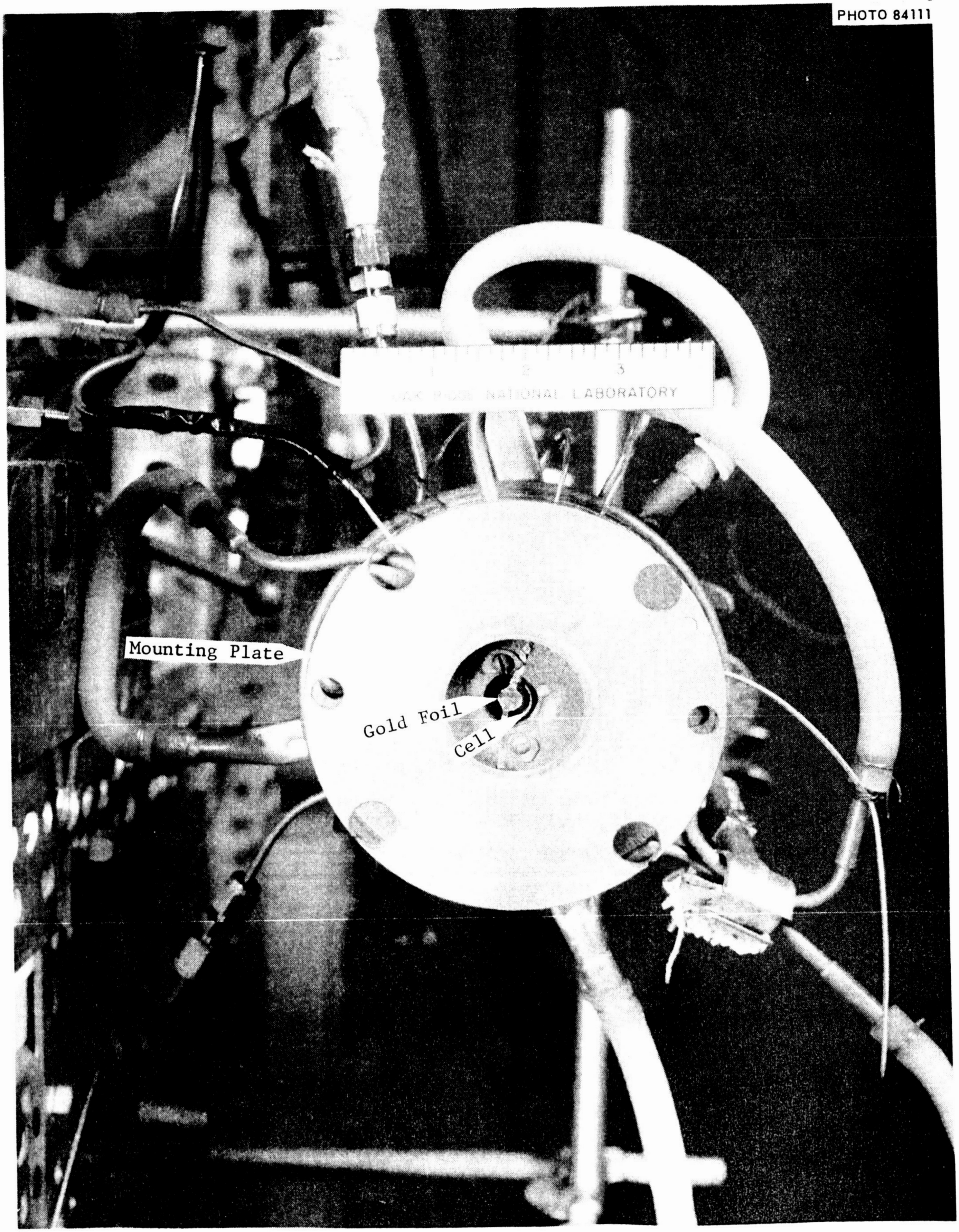

Fig. 6. Static Cell Mounted for Irradiation.

ORNL DWG. 66-6950

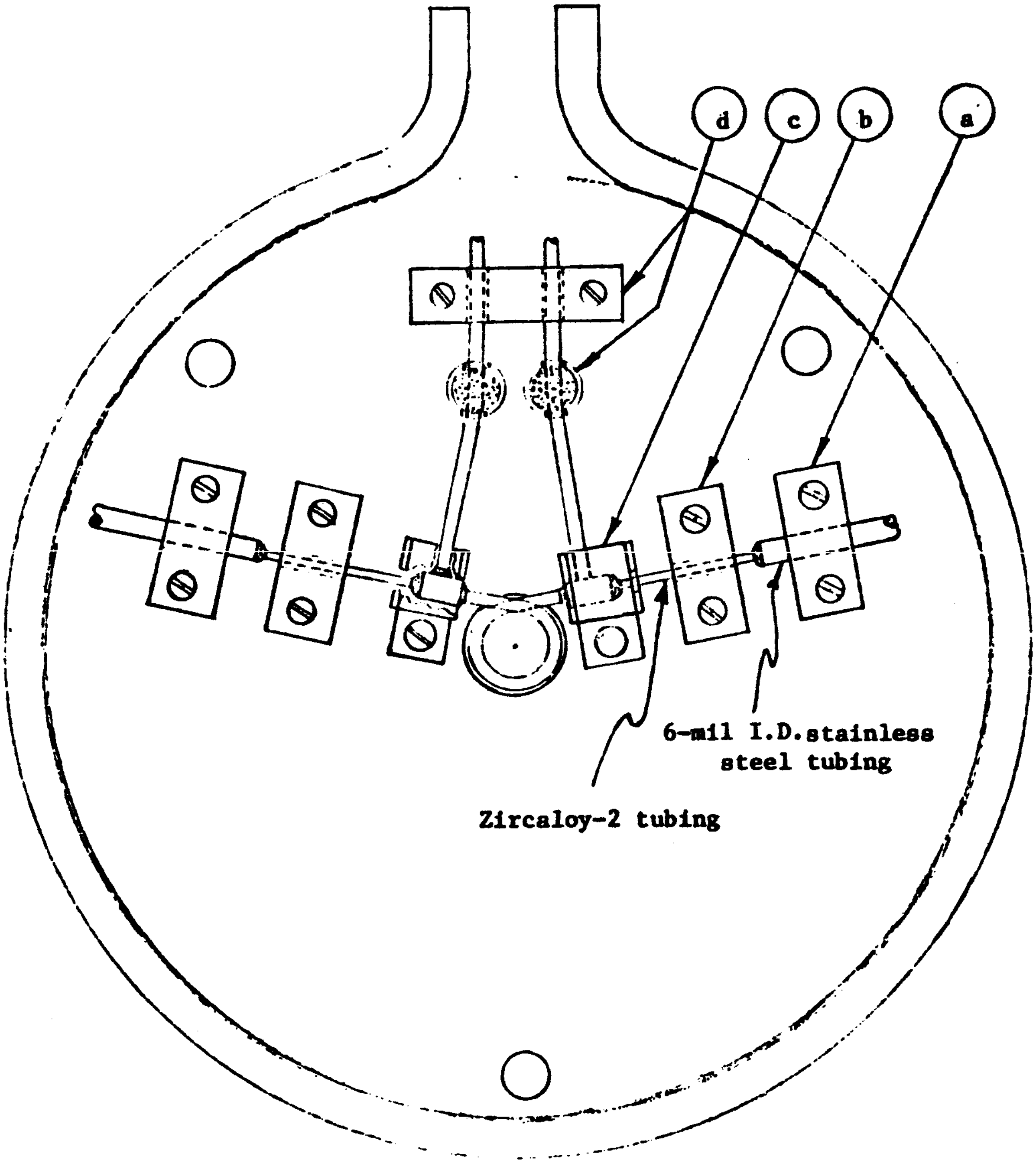

Fig. 7. Mounting Arrangement for Cell-4.

ORNL DWG. 66-1175

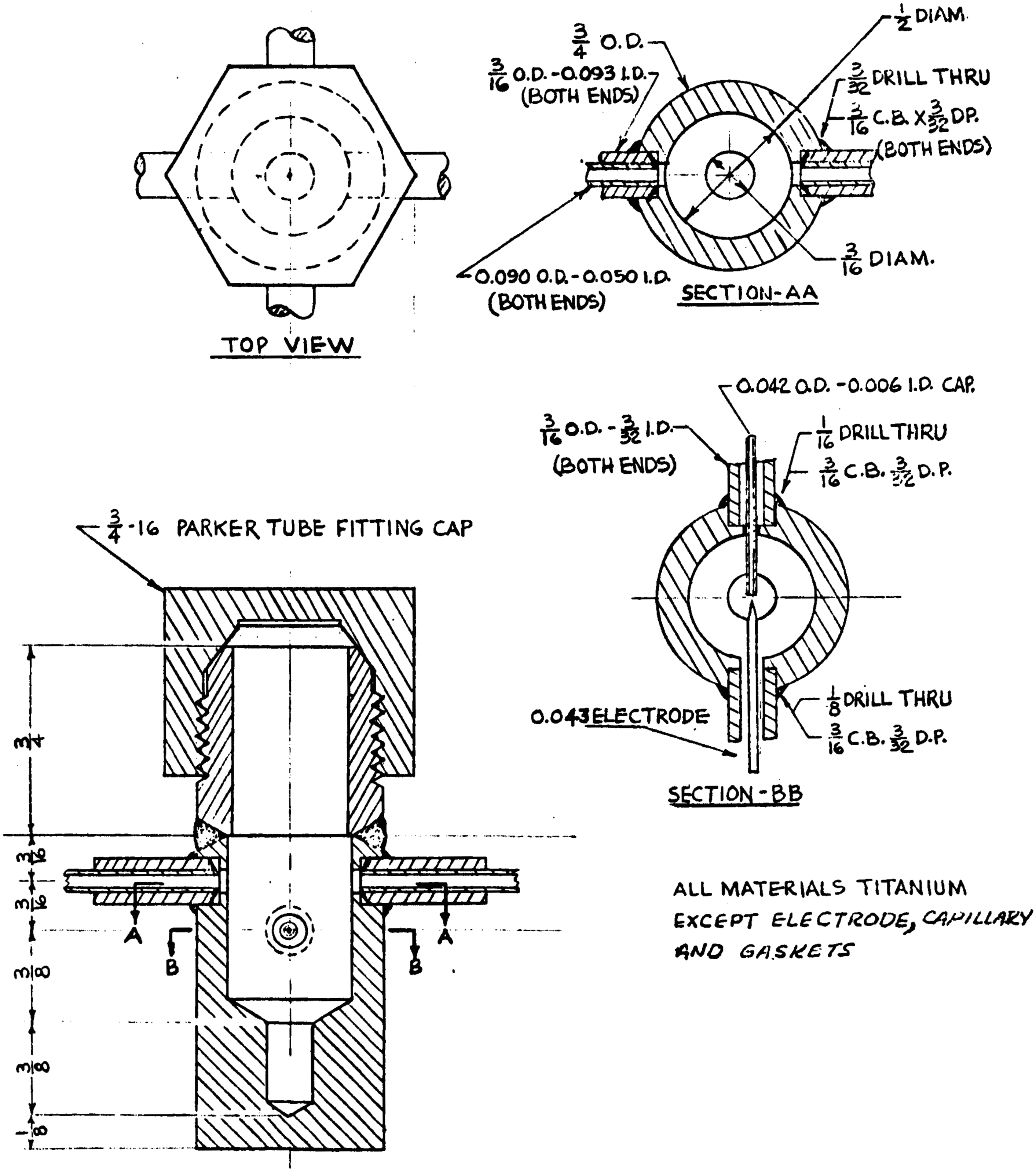

Fig. 8. Sample Collection Chamber.

Appendix I

Methods and Information for Estimations of Uniformitv of Dose Across Thickness of Cell

I.1 Range of 2 Mev Electrons

Values for ranges of 2 Mev electrons in several materials are set forth in Table I-1. These were taken or estimated from information reported by Nelms.[8]

I.2 Electron Energy Deposition vs. Fraction of Range

Relationships between the fraction of the energy absorbed from an electron beam and the fraction of the range traversed in the absorber are shown in Fig. I.1. Those for Al, H_2O and Au were deduced from reported information on ionization density vs. depth in absorber.[9-11] The relationships for stainless steel and Zr were estimated assuming (1) that the difference between the illustrated relationships for Al and Au results from the strong scattering of electrons by Au, and (2) that the fraction F_x of the energy absorbed in stainless steel or Zr at a given fraction of the range can be estimated roughly by,

$$F_x = (F_{Au} - F_{Al})\frac{S_x}{S_{Au}} + F_{Al} \qquad \text{(I-1)}$$

where F_{Au} and F_{Al} are the fractions of the energy absorbed in Au and Al at the given fraction of the range, and S_x and S_{Au} are the fractions of 2 Mev electrons which are backscattered from stainless steel or Zr and from Au.* Backscattering data reported by Wright and Trump[12] were employed.

---

*Backscattering from Al is small and was neglected in these rough estimates.

I.3 Estimation of Effects of Absorbers in Front of Solution Target

For these estimates, it was assumed that absorption in materials in front of the solution could be treated as though they were comprised of water of such thickness that the fractions of electron energy absorbed in a given material and water are equal. For example, absorption of 0.3 of the electron energy in zirconium at 0.15 of the range in zirconium was regarded as equivalent to absorption in water at 0.23 of the range in water.

Table I.1 Range of 2 Mev Electrons in Several Materials

Material	Range		
	(g/cm^2)	(cm)	(mils)
H_2O	.958	.958	377
Zirconium	1.52	.233	91.7
Aluminum	1.20	.444	175
Stainless Steel	1.30	.161	63.4
Platinum	1.8	.084	33
Iron	1.34	.170	66.9
Copper	1.24	.139	54.7
Titanium	1.26	.280	110
Gold	1.8	.093	37

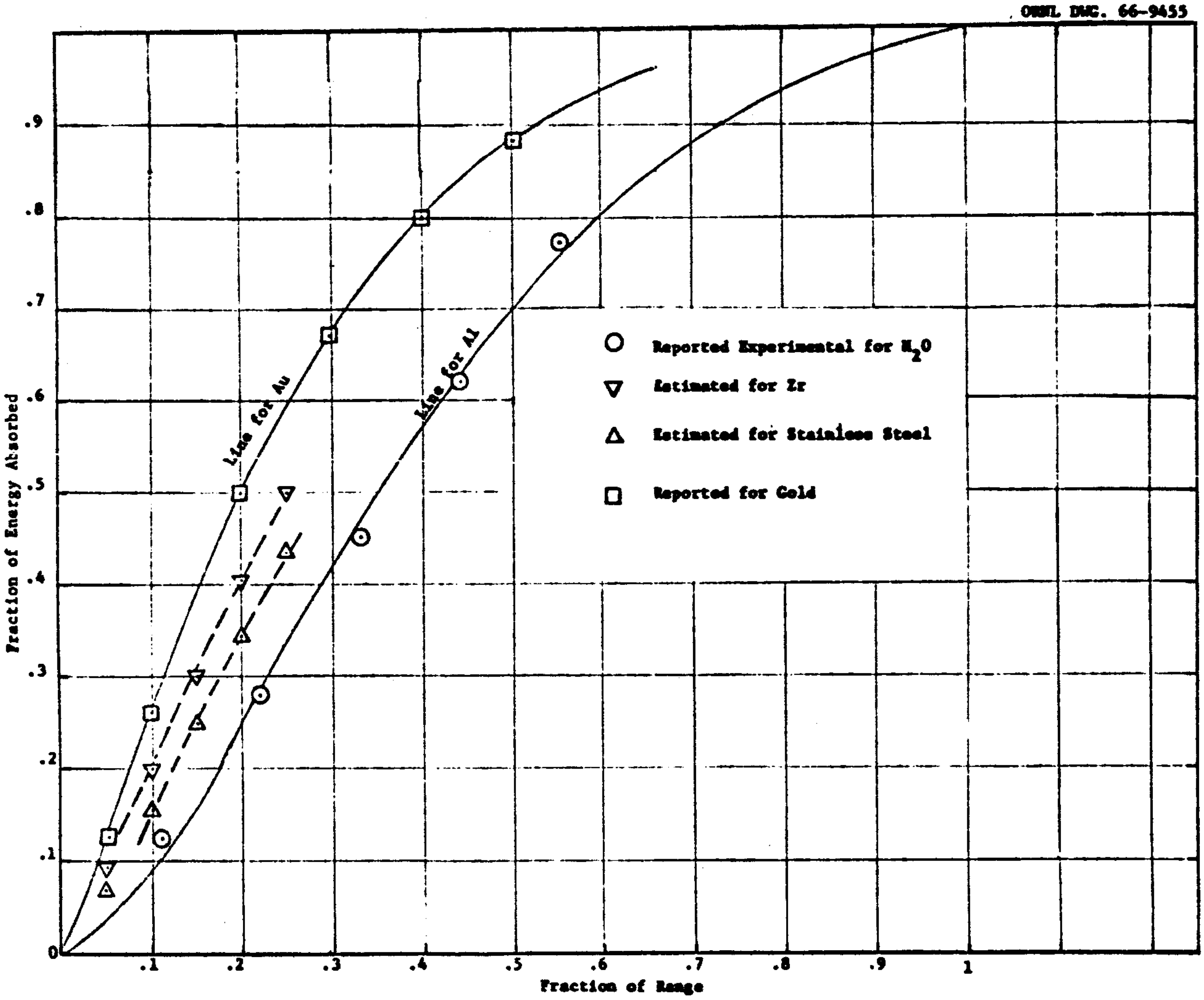

Fig. I.1. Fraction of β-Energy Absorbed vs. Fraction of Range Traversed.

Appendix II

Results of Measurements of Beam Intensity and Uniformity Without Scatterer

Values for current density on separate annular rings are shown in Fig. II.1. These were calculated from the observed effects of changing hole size and the separation between collector and Van de Graaff window. The curved lines were drawn arbitrarily thru the values for 3.62 cm. No lines were estimated for the fewer data at 2.99 cm. The listed values for expected power densities in solution were calculated using information discussed in Section 4.1. Possible backscattering of electrons into the solution was neglected in these estimates.

ORNL DWG. 65-7587

Full Lines - Collector 3.62 cm from Van de Graaff window

Dashed Lines - Collector 2.99 cm from Van de Graaff window

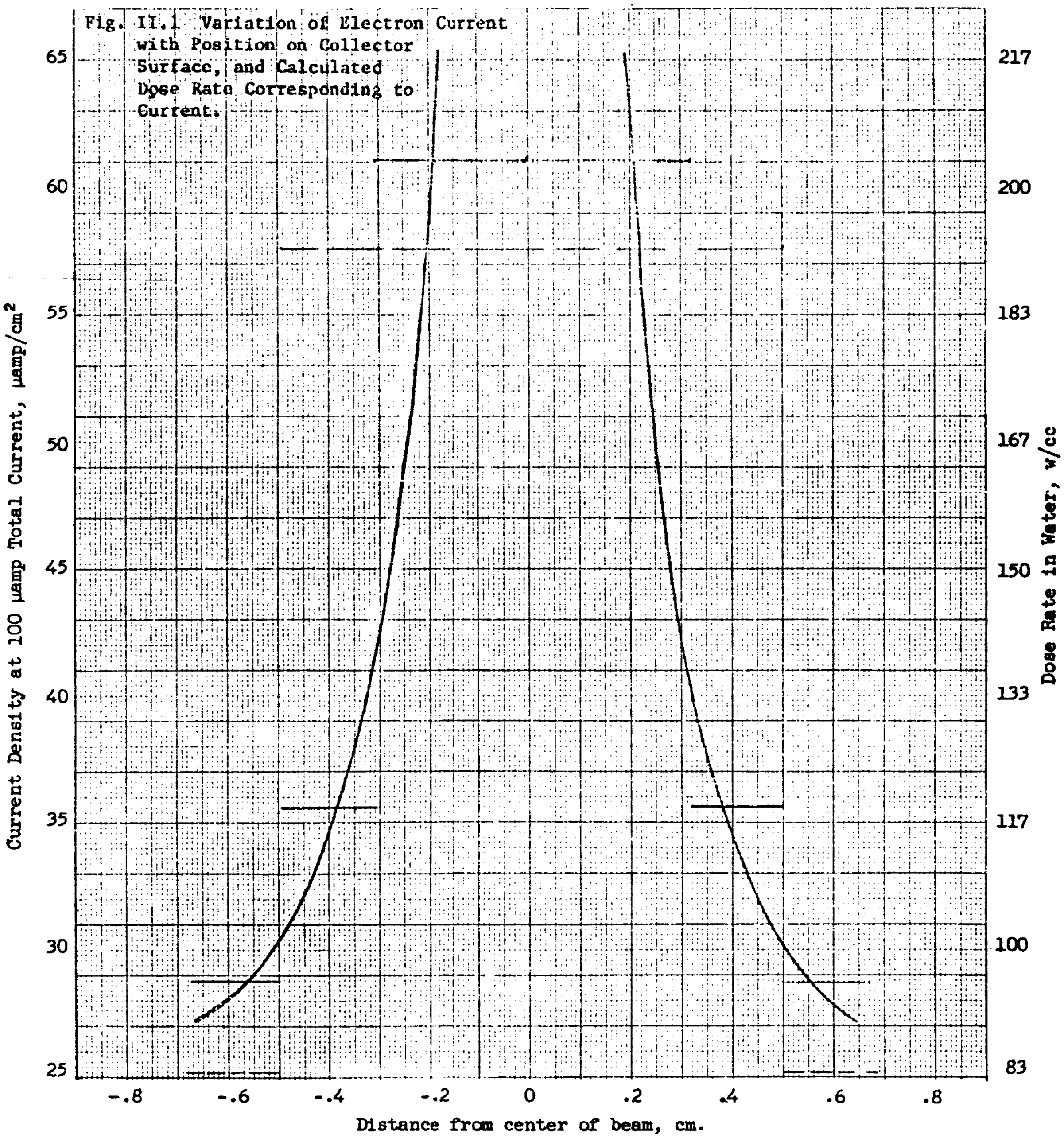

Fig. II.1 Variation of Electron Current with Position on Collector Surface, and Calculated Dose Rate Corresponding to Current.

Appendix III

Beam Intensity and Uniformity with Beam Scatterer

(Test Conditions and Results)

The experimental conditions and scattering materials and locations are listed in Table III.1. Total currents to the pins and to other collector surfaces are also listed in Table III.1. The average of the currents to the pins within each circle is listed in Table III.2* together with calculated values for the average current density at 100 μamps total current and for the average power density at the normalized current density. (Neglecting backscattering). The results for some of the experiments at 2.91 and 2.27 cm between collector and Van de Graaff window are plotted in Figs. III.1 and III.2, respectively. An additional plot in which the diameter of the pins is shown is given in Fig. III.3.

---

*Differences between the currents to individual pins within a circle were small.

Table III.1 Experimental Conditions and Beam Currents Employed in Beam Monitor Experiments

Experiment No.	Distance from Window[a] (cm)	Beam Current[b]			Scatterer		
		Pins[c] (μamp)	Other[d] (μamp)	Total (μamp)	Material	Thickness[e] (mils)	Distance from Collector (cm)
1	2.27	5.0	33.5	38.5	None	--	---
2	2.27	4.2	33.5	37.7	Au	1.0	0.32
3	2.27	3.7	33.5	37.2	Au	1.0	0.48
4	2.27	3.2	33.5	36.7	Au	2.0[f]	0.32
5	2.27	4.2	33.5	37.7	Al	8.0	0.48
6	2.91	4.2	33.5	37.7	None	--	---
7	2.91	3.6	33.5	37.1	Au	1.0	0.32
8	2.91	3.1	33.5	36.6	Au	1.0	0.48

a. Distance between window and surface of collector.

b. Electron voltage was 1.95 Mev.

c. Total current to pins.

d. Current to remainder of collector and to window.

e. Scatterers were centrally located and were 0.60 cm diameter except as noted.

f. Diameter was 0.55 to 0.60 cm.

Table III.2 Results of Measurements of Current to Pins

Experiment No.	Circle No.[a]	Average Current Per Pin[b] (μamp)	Normalized Average Current Density[c] (μamp/cm^2)	Normalized Power Density in Solution[d] (w/cc)
1	0	.76	89	297
	1	.49	58	193
	2	.36	42	140
	3	.17	20	67
2	0	.50	60	200
	1	.34	41	137
	2	.40	48	160
	3	.24	29	97
3	0	.36	44	147
	1	.32	39	130
	2	.32	39	130
	3	.23	28	93
4	0	.27	33	110
	1	.24	30	100
	2	.33	41	137
	3	.21	26	87
5	0	.59	71	237
	1	.38	46	153
	2	.36	43	143
	3	.22	26	87
6	0	.54	65	217
	1	.40	48	160
	2	.31	37	123
	3	.22	26	87
7	0	.41	50	167
	1	.27	33	110
	2	.35	43	143
	3	.22	27	90
8	0	.25	31	103
	1	.25	31	103
	2	.29	36	120
	3	.25	31	103

---

a. Radii of circles: 1. 0.277 cm, 2. 0.437 cm, 3. 0.595 cm.

b. At conditions during measurements as listed in Table III.1.

c. Calculated average current density at 100 μamp total assuming a pin area of .0221 cm^2.

d. Calculated from normalized current density assuming maximum rate of energy absorption but neglecting backscattering.

ORNL DWG. 65-8430

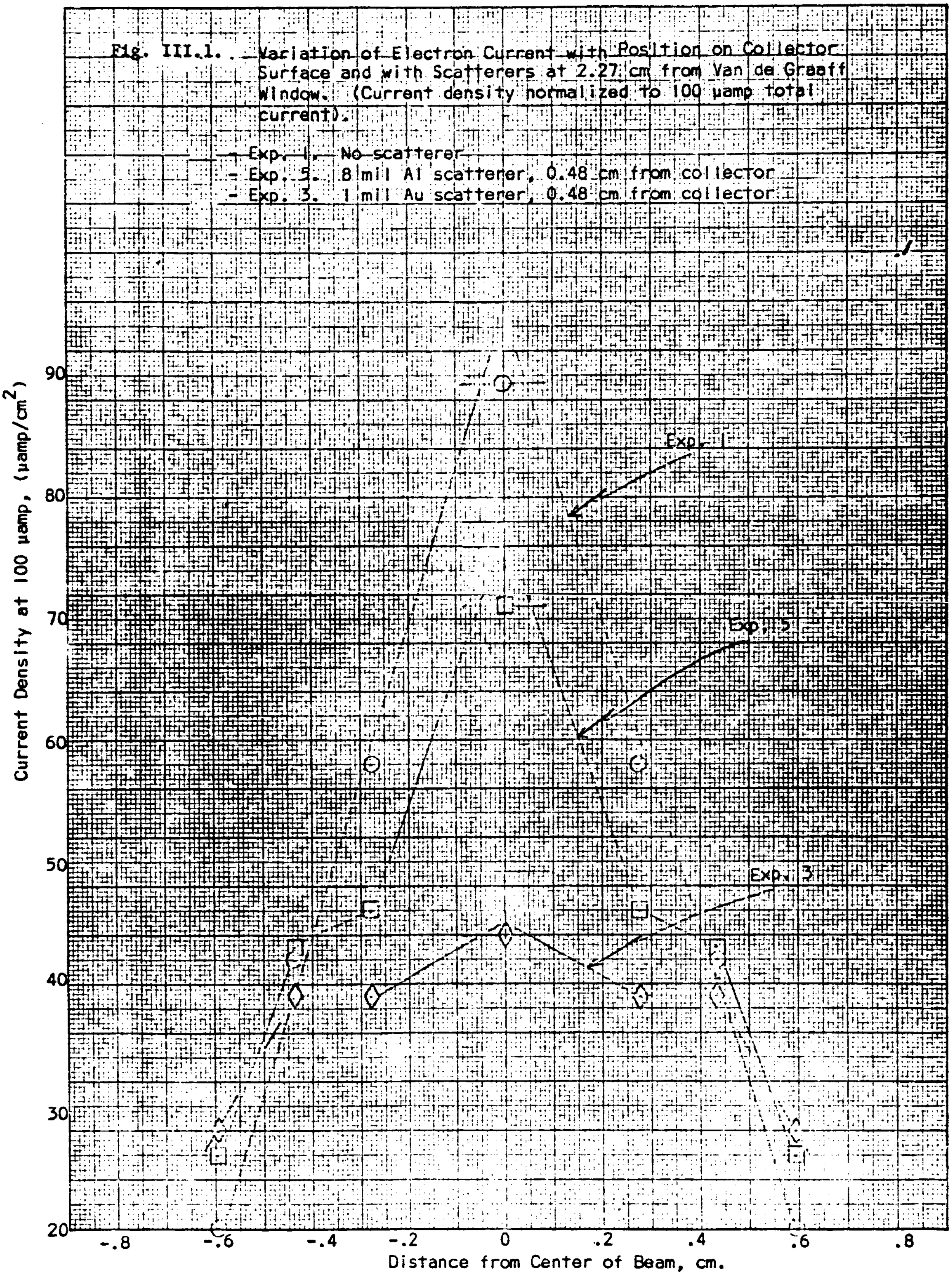

Fig. III.1. Variation of Electron Current with Position on Collector Surface and with Scatterers at 2.27 cm from Van de Graaff Window. (Current density normalized to 100 μamp total current).

ORNL DWG. 65-8429

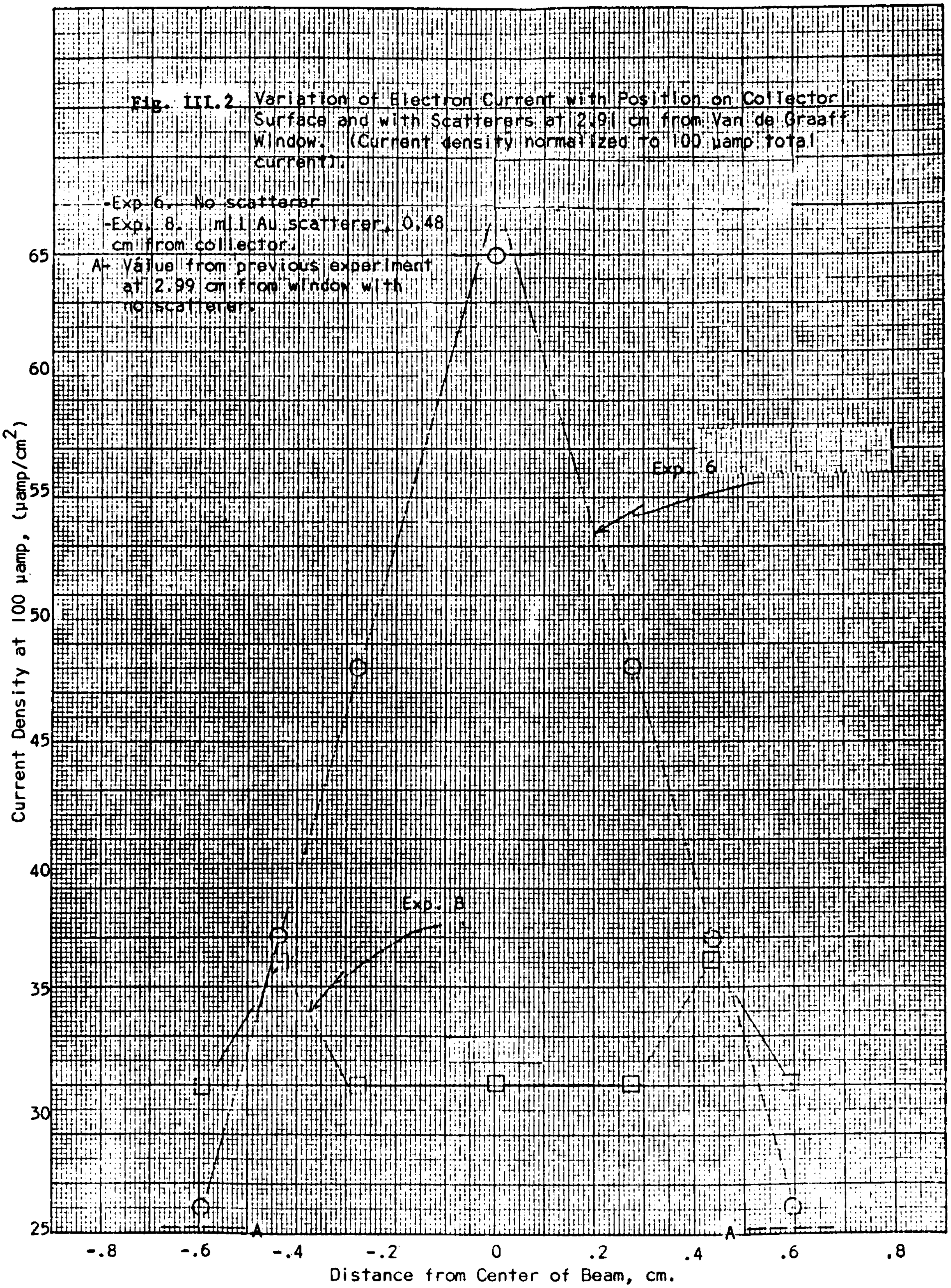

Fig. III.2 Variation of Electron Current with Position on Collector Surface and with Scatterers at 2.91 cm from Van de Graaff Window. (Current density normalized to 100 μamp total current).

ORNL DWG. 65-8431

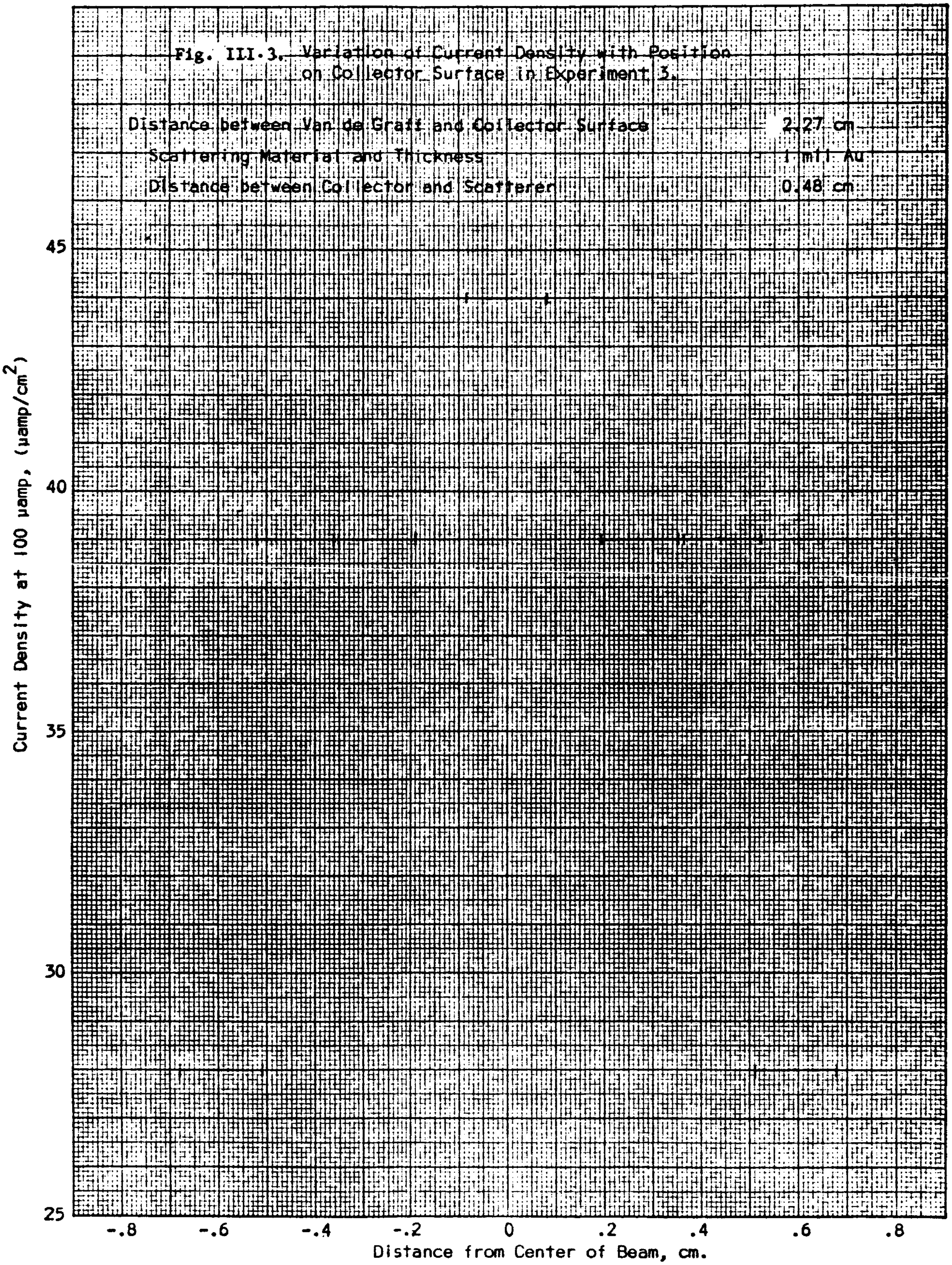

Fig. III-3. Variation of Current Density with Position on Collector Surface in Experiment 3.

Distance between Van de Graff and Collector Surface	2.27 cm
Scattering Material and Thickness	1 mil Au
Distance between Collector and Scatterer	0.48 cm

Appendix IV

Dosimetry Measurements in Mock-ups of Static and Dynamic Cells

IV.1 Introduction

We determined the rates of deposition of electron energy in dosimetry solutions contained in mock-ups of the static and dynamic cells. The objectives of these determinations were (1) to establish that approximately uniform power densities of about 150 w per cc of solution could be obtained within experimental systems with the available electron current of 100 μamps, maximum, and (2) to establish the relationship between total beam current and power density in $CdSO_4$ solutions for the experimental static cell.

The design of the dynamic mock-up experiments provided for batch-type irradiations of the dosimetry solution to total doses in the range of 10^{23} ev/ℓ (1.7 megarads). Smaller doses were not practical because the minimum current and exposure times which could be measured reliably and/or conveniently were about 1 μamp (about 9 x 10^{21} ev/ℓ/sec) and 10 sec, respectively. This dose range is far in excess of that which can be used with the Fricke (ferrous sulfate) dosimeter. However, it is within the range which can be measured with the ceric sulfate dosimeter, and, accordingly, the latter was used.

The static cell mock-up was a flow-thru system, and, thus, lesser doses might have been used. However, it was convenient to use the solution and dose range which were used with the dynamic mock-up and this was done. The dose rates employed with the static mock-up experiments ranged up to 15 megarads per sec while those with dynamic mock-up were in the range of 0.15 megarads per sec.

Taimuty and coworkers[13] investigated ceric dosimetry in the dose range 10^5 to 10^7 rads* using ceric ion concentrations of 0.01 to 0.05 M with doses which produced 20 to 80% reductions of the Ce^{+4}. They showed that the value of $G(Ce^{+3})$ does not change with (Ce^{+4}), and is independent of dose rate up to 2×10^6 rads/sec. They also pointed out that the theoretical limit for dose rate independence is $\sim 10^{11}$ rads/sec. A small temperature dependence was noted as shown in Fig. IV.1 where we have plotted their reported G-values. Their solutions were composed of ceric sulfate (G. F. Smith) or ceric ammonium sulfate (Baker and Adamson) dissolved in 0.4 M H_2SO_4 solutions.

Some organic impurities affect the value of $G(Ce^{+3})$. However, it has been found[14] that heating the test solution (~80°C) overnight before use produces a substantial reduction in the possibility of encountering an effect of organic impurities. Presumably, the impurities are removed by reaction with Ce^{+4} during the heating.

Some authors recommend[13] calibration against an absolute standard to establish $G(Ce^{+3})$ for the particular solution composition used.

IV.2 Theory

IV.2.1 Reduction of Ce^{+4} Under Irradiation

Since the dosimeter solutions are strongly acid, the e^-_{aq} reacts with H^+ to form H, and the general radiolysis equation for low LET radiations (β and γ) can be written,

$$H_2O \rightarrow H_2, H_2O_2, H, OH.$$

---

*10^7 rads equal approximately 6×10^{23} ev/ℓ and 100 w,sec/cc in water.

The reducing reactions are thought to be,[15,16]

(1) $H + Ce^{+4} \rightarrow Ce^{+3} + H^{+}$

(2) $H_2O_2 + Ce^{+4} \rightarrow Ce^{+3} + H^{+} + HO_2$

(3) $HO_2 + Ce^{+4} \rightarrow Ce^{+3} + H^{+} + O_2$.

The oxidation reaction is,

(4) $OH + Ce^{+3} \rightarrow Ce^{+4} + OH^{-}$.

Assuming that no other reaction is of importance, the yield of Ce^{+3} is given by,[17]

(5) $G(Ce^{+3}) = 2G_{H_2O_2} + G_H - G_{OH}$.

Hydrogen and oxygen are evolved at rates corresponding to G_{H_2} and $G_{H_2O_2}$, respectively. (About 10 cc of H_2 and 16 cc of O_2 per liter per 10^6 rads).

The value of $G(Ce^{+3})$ obtained from Eq. 5 together with G values for H_2O_2, H and OH for 0.4 M H_2SO_4 solution is near 2.35[17] whereas, in practice, Taimuty and coworkers found $G(Ce^{+3})$ equal to 2.50 (Fig. IV.1). No reported explanation for this difference has been found. However, our considerations led us to conclude that the difference results from an increase in the effective yield of H caused by reaction of O_2 and Ce^{+4} with H within the spur. Using data reported by Hochanadel and Ghormley,[18] we calculate that G_{H_2} would be reduced 0.052 by dissolved oxygen at a concentration of 8.5×10^{-4} M (2/3 atm) and an additional 0.023 by 0.01 M Ce^{+4}. These values corresponded to an increase in G_H of 0.15. The amount by which the G_H would be increased was expected to depend upon the one-third power of the concentration of O_2 and of Ce^{+4} so that other concentrations which prevailed in the experimental work would have produced slightly different enhancements of G_H. For example, the increase resulting in 0.05 M Ce^{+4} would be expected to be 0.076 as compared with the above mentioned increase of 0.046 in 0.01 M Ce^{+4}. Since it appears likely that dissolved O_2 was present in many of the experiments of Taimuty et al., at a pressure of about 1/5 to more than 2/3 atms,* the difference between the experimental and theoretical values of $G(Ce^{+3})$ can probably be satisfactorily explained.

The explanation for the slight decrease in $G(Ce^{+3})$ with increasing temperature has not been established. It can be speculated that decreased solubility of gases at the elevated temperature accounts for part of the temperature effect.

It should be noted the dosimeter solutions are normally open to the atmosphere during irradiation.[13,15] Pressurization would result in a build-up of concentration of H_2 and O_2 which might be sufficient to alter $G(Ce^{+3})$. An effect of H_2 would be exercised thru reaction (6),

$$(6) \quad H_2 + OH \rightarrow H + H_2O.$$

As mentioned in Section IV.1, dose rates up to 15 megarads per sec were used in our experiments while the dose rate independence of $G(Ce^{+3})$ has been established to only 2 megarads per sec. However, we found no theoretical reason to expect a different value for $G(Ce^{+3})$ at the higher dose rate.

---

* Oxygen produced during irradiation plus dissolved air initially present.

IV.2.2 Effect of Degradation of Electron Energy on G(Ce^{+3})

In planning the dose rate measurements using dosimeter solutions, a question can be raised as to whether the changes in LET, and the accompanying changes in G-values, which result from electron energy degradation produce significant effects on overall G-values. In our work with ceric dosimeter solutions, the question was whether any changes in LET and G-values were sufficient to significantly alter the average G(Ce^{+3}) from that expected for 0.02 ev/Å radiations (cobalt γ-rays and electrons with energies greater than 0.4 Mev). An answer to this question was obtained for each of the three different systems listed below:

1. System in which all of the electron energy is absorbed in solution.

2. System comprised of a layer of solution sandwiched between a Zircaloy-2 window and a Zircaloy-2 backscatterer of infinite thickness. The thicknesses of the solution and window were assumed to be 0.3 cm and 5 mils. This absorption system is comparable to that prevailing in the planned dynamic cell.

3. System similar to No. 2 but with solution and window thicknesses of 0.054 cm and 10 mils. This absorption system is comparable to that used in the static cell.

Information presented by Allen for: (1) the LET of electrons in water as a function of energy,[19] and (2) the value of G(Ce^{+3}) as a function of LET[19] was employed in the evaluation of the average G(Ce^{+3}) for system No. 1. The evaluations of systems 2 and 3 employed, additionally, information in Appendix I for energy absorption vs fraction of range traversed, and data reported by

Trump and Wright[12] for: (1) the fraction of electrons backscattered, (2) the fraction of incident energy backscattered, and (3) the ratio of average energy per backscattered electron to energy of primary electron.

The method of evaluating the effects of energy degradation for system 1 can be seen by reference to Table IV.1 in which lists are given of several parameters employed in the evaluation. The results show that the average $G(Ce^{+3})$ may be about 1% greater than that expected when all of the energy is deposited by electrons with energies greater than 0.4 Mev. This increase is less than the expected overall uncertainty in the measurements.

The results for system 2 (Table IV.2) show that about 65% of the electrons are lost when the electrons strike the back plate in the first pass, and that 95% of the energy of all electrons is absorbed by the time backscattered electrons are absorbed in the solution, it can be estimated that 0.07 of the initial electron energy of 2 Mev is absorbed in solution from electrons with energies < 0.4 Mev. At the same time the total fraction of the initial electron energy which is absorbed in solution is 0.55. Accordingly, the fraction of energy dissipation in water due to electrons with energies < 0.4 Mev is 0.13. Considerations of the type described above for system 1 then show that the expected increase in $G(Ce^{+3})$ resulting from the presence of low energy electrons is well below 1%.

The results for system 3 showed that about 90% of the electrons are absorbed in the back wall and that the incident energy on striking the wall is > 0.4 Mev. The fractions of the energy absorption in solution from electrons with energies below and above 0.4 Mev are 0.17 and 0.83. Again by comparison

Table IV.1 Evaluation of Average G(Ce^{+3}) for Complete Absorption of Energy of 2 Mev Electrons in Water (System 1)

Electron Energy Range (Mev)	Fraction of Initial Electron Energy	Average LET[a] (ev/A)	G(Ce^{+3})[b]	Product of Fraction of Energy and G(Ce^{+3})
2.0 to 0.4	0.80	0.020	2.37	1.89
0.4 to 0.3	0.05	0.021	2.37	0.119
.3 to .2	0.05	0.024	2.39	0.120
.2 to .1	0.05	0.036	2.49	0.124
.1 to .08	0.01	0.044	2.55	0.025
.08 to .06	0.01	0.053	2.60	0.026
.06 to .04	0.01	0.068	2.69	0.027
.04 to .02	0.01	0.098	2.94	0.029
.02 to 0	0.01	-	3.2[c]	0.032
		Average G(Ce^{+3})		2.39

a. From ref. 6, p. 6

b. From ref. 6, p. 54

c. Assuming the maximum value of G(Ce^{+3}).

Table IV.2 Energy Absorbed from Electrons of Different Energies in Static and Dynamic Systems and Effects on G(Ce^{+3})

	Dynamic	Static
Fraction of Initial Energy Absorbed in solution	0.55	0.12
Fraction of Initial Energy Absorbed from Electrons with Energies:		
< 0.4 Mev	(.35)(.2) = 0.07	(.1)(.2) = 0.02
> 0.4 Mev	0.48	0.10
Fraction of Energy Absorption from Electrons with Energies:		
< 0.4 Mev	0.13	0.17
> 0.4 Mev	0.87	0.83
Percentage Deviation of G(Ce^{+3}) from that of 0.02 ev/Å	< + 1	< + 1

with the results of considerations described for system 1, the expected increase in G(Ce^{+3}) resulting from low energy electrons is less than 1%.

IV.3 Method

IV.3.1 Preparation of Stable Solutions

The composition and density of dosimeter solutions employed in this work are listed in Table IV.3. These solutions were made using triply distilled water, Fisher $Ce(SO_4)_2 \cdot 2(NH_4)_2 SO_4 \cdot 2H_2O$, and concentrated H_2SO_4. The solutions were heated overnight at ~80°C before use. No precipitation occurred during heating or during subsequent irradiation.

Solutions containing 0.4 M H_2SO_4 were also prepared during preliminary work, but precipitation from these solutions occurred during heating and/or during irradiation. Ceric sulfate, $H_4Ce(SO_4)_4$, was also tested in these preliminary experiments. Precipitation was always encountered. No alteration of G(Ce^{+3}) is expected to result from the use of 0.7 M H_2SO_4 since the G-values of the radiolytic species involved (Eq. 5) are substantially the same in 0.7 and 0.4 M H_2SO_4.[20]

Table IV.3 Composition and Density of Dosimeter Solutions

Solution No.	Solution Concentration (M)		Density (g/cc at 25°C)
	$Ce(SO_4)_2 \cdot 2(NH_4)_2SO_4 \cdot 2H_2O$	H_2SO_4	
A	0.01	0.7	1.042
B	0.06	0.7	1.062

IV.3.2 Evaluation of G(Ce^{+3})

Values of G(Ce^{+3}) for our solutions were determined by exposing samples in the Chemistry Division cobalt source where the dose rate in water is accurately known.[21] Dose rates in the dosimeter solutions were obtained using our calculated ratios of γ-ray absorption coefficients in the solutions to that in water. The information and an illustration of the method used for evaluation of this rate for solution A are set forth in Table IV.4. The value for the ratio in this case was 1.039 as shown in the table. The similarly evaluated ratio for solution B was 1.058.

Doses of about 2 x 10^6 rads were used in these calibrations. These required about 85 min of exposure.

Table IV.4 Evaluation of Relative γ-ray Absorption Per Unit Volume in Dosimeter Solution and Water

Species	Concentration		Gamma Energy Absorption Coefficient[a]	Product of Absorption Coefficient and Density
	(M)	(g/cc)	(cm^2/g)	(1/cm)
Ce	.01	.0014	.03[b]	.000042
S	.74	.0237	.0280	.00066
O(except H_2O)	2.96	.0474	.0280	.00133
N	.04	.00056	.0280	.000016
H(except H_2O)	1.56	.00156	.0555	.000087
H_2O		.967	.0311	.03007
Sum of products of absorption coefficient and density				0.0322
Ratio energy absorption coefficient (1/cm) in solution to that in H_2O				1.039

[a] NBS Handbook 62 (1956), p. 16.

[b] Estimated

IV.3.3 Evaluation of Electron Doses in Water

The rate of deposition of electron energy in a dosimeter solution was determined in our work from measured values of the rates of formation of Ce^{+3} in the solution together with the appropriate measured value of $G(Ce^{+3})$. The rate of energy deposition in water was then evaluated from comparisons between the electron range in H_2O and that in the solution. Values for the ranges in solutions A and B and values for the fractions of the range presented by a 3 mm thickness of solution are listed below.

	Solution A	Solution B
Range of 2 Mev electrons	0.971 g/cm^2	0.988 g/cm^2
Fraction of range in 3 mm of solution	0.321	0.323

Fraction of range in 3 mm of H_2O, 0.314.

Other information employed in evaluating the range in solution A is presented in Table IV.5.

Table IV.5 Evaluations of Range of 2 Mev Electrons in Dosimeter Solution A.

Species	Range of 2 Mev Electrons[a] (g/cm^2)	Concentration (g/cc)	Weight Fraction of Species	Product of Weight Fraction and Range (g/cm^2)
Ce	1.6	0.0014	0.0013	0.0021
S	1.19	0.0237	0.0227	0.0270
O(except H_2O)	1.11	0.0474	0.0455	0.0505
N	1.10	0.00056	0.00054	0.00059
H(except H_2O)	0.471	0.00156	0.0015	0.00071
H_2O	0.958	0.967	0.929	0.890
Sum of products of weight fraction and range				0.971
Range of 2 Mev electrons in solution				0.971

a. Taken or estimated from information in NBS Circular 577, 1956.

Using these range values and referring to Fig. I.1, Appendix I, it can be shown that the ratio of the rate of electron energy absorption in either solution to that in water is 1.030.

IV.4 Equipment and Procedures

IV.4.1 Static Mock-up

Fig. IV.2 is a photograph of the mock-up assembly which consisted of one coil of Zircaloy-2 tubing (0.023 in. ID x 0.030 in. OD) surrounded by a stainless steel cooling jacket (0.062 in. OD x 0.051 in. ID). A 1/8 in. thick brass shield plate with a center hole was used to define the area of irradiation. For these measurements, one end of the Zircaloy-2 test loop was connected by means of titanium tubing to a titanium tank containing ceric solution. The tank was located outside the Van de Graaff room. The other end of the loop was also connected to titanium tubing. Test solution was conducted to a graduated cylinder or to discard through this tubing. The joints between the titanium and the Zircaloy-2 tubing were made by slipping the Zircaloy-2 into the drilled ends of the titanium and then sealing with epoxy cement.

A dose rate measurement was carried out as follows: The equipment was assembled, and the cooling jacket around the test tube was connected to a tap supplying cold water at a pressure of about 61 psi. Cold tap water was also passed thru the cooling coil around the mounting plate. Solution flow thru the test tube was then initiated, and the Van de Graaff was started. When the total beam current was at the desired level, the delivery tube was moved so that the solution was collected in a graduated cylinder. After collection of a sample of appropriate size, the delivery tube was moved so that the solution discharged to waste. The Van de Graaff was then stopped, and the sample in the cylinder was removed for analysis. Control experiments in which the same procedure was followed except that the test cell was shielded from the electron beam were carried out immediately following some of the experiments. Control tests were also carried out using the same procedure except that the Van de Graaff was not operated.

Solution A was used in all of these experiments, and no attempt was made to exclude air from the solution. Total beam currents of about 80 to 95 and 45 μamps at 2 Mev were tested. The flow rate was adjusted so that the expected reduction of Ce^{+4} amounted to about 20 to 30% (about 0.12 cc/sec at 95 μamp). Adjustment of the flow was accomplished thru adjustment of helium pressure over the solution within the tank.

Solution analyses were accomplished by titration with a standard.

The temperatures of the inlet and outlet tubes attached to the cooling jacket were determined by means of thermocouples which were wired and taped to the tubes about one-half inch above the points of attachment to the mounting plate.

Values of certain parameters of the static cell mock-up which were employed in interpretations of results are listed in Table IV.6. Additional information is given below under numbers corresponding to numbered items in the table.

2. The inlet temperature before irradiation was 23.6°C. Presumably, radiation heat was conducted to the water thru the connection to the mounting plate and at other points of near contact.

4. From the Hausen equation for flow in the transition region.

5. Based on Nusselt number in 4.

6. Assuming reported[22] values for rates of heat flow from the test tube.

7. Each type of measurement was made on a straight length of tubing. Measurement type c was also made with the tube after fabrication into the cell. The results of the type c measurements for the straight and coiled pieces were the same. The results showed that Hg did not fill the tubing completely; probably because of the rough oxide surface.

12. Taking heat flow from the wall into account.

The temperature of a particular experiment may have differed from this value by ± 2 or 3°C. Since the value of G(Ce^{+3}) is not very sensitive to temperature, no attempt was made to obtain more precise temperatures.

It may be noted that the duration of irradiation of a sample was computed from knowledge of the I.D. of the Zircaloy-2 test tube and from the measured volume of solution collected during a known period. As stated previously, the flow rates were adjusted so that the amount of Ce^{+4} reduced during irradiation would amount to less than about 40% of that initially present. Consideration was given to the possibility that the duration of irradiation in relatively low velocity portions of the channel would exceed that required to completely reduce the Ce^{+4} and thus alter the average amount of reduction from that which would occur with good mixing. It was recognized that if the flow was perfectly streamline with no mixing or diffusion, then the total dose in about 20% of the solution would exceed that required for complete reduction by factors ranging up to 2 in some experiments. The dose in the remaining 80% of solution would be less than that required for complete reduction.

Consideration of the reactions which would occur among the radiolytic products in the temporary absence of Ce^{+4} led to the conclusion that the average

Table IV.6 Values of Certain Parameters of Static Cell Mock-Up

	Jacket Coolant System		
1.	Velocity of flow thru 7 mil annulus (at 61 psi ΔP and 23°C)		19 fps
2.	Approximate temperature of coolant water at beam current of 82 μamps	Inlet	27°C
		Outlet	29°C
3.	Reynold's number		2,230
4.	Nusselt number		9.50
5.	Film coefficient on outer surface of test tube		3,350
6.	Approximate temperature of test tube surface		36°C
	Zircaloy-2 Test Tube		
7.	ID		
	a. From microscopic measurements of bore		.0574 cm
	b. From weight and OD measurements		.0574 cm
	c. From measurements of weight of Hg to fill tube		.0533 cm
8.	Length of irradiated portion		4.45 cm
9.	Average velocity of solution at 0.12 cc/sec		46 cm/sec
10.	Reynold's number at 46 cm/sec and 30°C		330
11.	Approximate temperature at inlet solution at 82 μamps		27°C
12.	Approximate temperature of solution at 150 w/cc and flow rate of 46 cm/sec		35°C
	Titanium Tube Joining Cell to Sample Collector		
	ID		0.058 cm
	Length		150 cm
	Residence time of fluid at volume flow rate of 0.12 cc/sec		3.3 sec
	Pressure drop at volume flow rate of 0.12 cc/sec		7.8 psi

amounts of reduction were not significantly different from those which would occur with good mixing. In the absence of Ce^{+4} the H which normally reacts with Ce^{+4} would react with O_2 to form H_2O_2 according to reactions 7, 8, and 9.

(7) $H + O_2 \rightarrow HO_2$,

(8) $HO_2 + HO_2 \rightarrow H_2O_2 + O_2$,

(9) $HO_2 + Ce^{+3} + H^+ \rightarrow Ce^{+4} + H_2O_2$.

If the H_2O_2 has nothing to react with immediately, it remains in the solution and eventually reacts with Ce^{+4} after some mixing has occurred. The net amount of reduction is not altered by the intermediate formation of H_2O_2. Since it is very unlikely that O_2 was exhausted, the presence of low velocity regions in the channel very likely did not affect the net amount of reduction.

It can also be assumed that the flow within the test tube loop was not perfectly streamline and that some mixing occurred as a result of secondary flow. The amount of mixing produced by the secondary flow is unknown, but it is considered likely that in the experiments employing the higher velocities, it was sufficient to effect at least one complete mixing during passage of solution thru the test loop. One complete mixing would be sufficient to prevent exhaustion of Ce^{+4} in any portion of the solution.

In general, it appears that any tendency for an effect on the average amount of reduction to result from the presence of low velocity regions will be least at the highest flow rates.

IV.4.2 Dynamic Mock-up

The dosimetry cells designed to simulate the electron energy absorption characteristics of the dynamic system were made from Zircaloy-2 cylinders with welded covers of zirconium. Inlet and exit tubes of Zircaloy-2 were provided for insertion and removal of dosimetry solutions. One of the cells (No. 2) is shown in Fig. IV.2. Dimensions are listed in Table IV.7

Table IV.7 Dimensions of Dosimetry Cells for Dynamic Mock-Up

	Cell No. 1	Cell No. 2
OD	1.30 cm	1.30 cm
ID	1.20 cm	1.20 cm
Window thickness	3 mils	11-12 mils
Bottom thickness	20 mils	3 mils
ID of attached tubing	0.0574 cm	0.0574 cm
Internal volume of tubing	0.021 cc	0.028 cc
Volume of cell (exclude tubing)	0.288 cc	0.301 cc
Average depth	0.255 cm (100 mils)	0.266 cm (105 mils)
Weight of cell (exclude tubing)	0.90 g	0.66 g

A measurement was carried out as follows. The cell was flushed and filled with ceric solution and then placed within the cavity of the mounting plate. It was then mounted at the Van de Graaff in an arrangement which included a one-eighth in. copper shutter between the beam window and the cell. The beam current was then adjusted, and the shutter opened for the desired length of time and then closed. The beam was then stopped and the sample removed for analysis. The cell was then recharged for the next experiment. Samples of the charged solutions were reserved for control analyses from time to time during a series of experiments. About 15 min elapsed between charging and removing the solution from a cell in a given experiment. An experiment was made prior to the radiation experiments to determine the rate of loss of Ce^{+4} by reaction with the cell walls.

Analyses of the small volumes of solution were accomplished by diluting the samples to about 10^{-4} M, and then analyzing spectrophotometrically.[13]

Solution A was used in all final experiments. The beam currents and exposure times were about 1 μamp and 10 sec. Solution B was employed in some preliminary experiments in which beam currents and exposure times of about 5 μamp and 20 sec were employed. About 30% of the solution was expelled from the cell during exposure in these preliminary experiments owing to heating in the cell walls and/or to gas evolution from the solution. No solution was lost from any of the final experiments.

Estimates of the temperature rise in a cell were made from considerations of energy absorption in the solution and walls along with the results of the experiments. As reported later, the results showed that 1 μamp total beam current corresponded to about 1.5 w/cc. The estimates of the temperature rise in the walls of cell No. 1 were made using Eq. 10,

$$(10) \quad T = T' + \frac{q'L}{KA}(1-\exp - \frac{KAt}{CL}),$$

which was derived by assuming that heat was not exchanged between solution and walls but was transferred from the wall to the sample holder thru an air gaps on the sides and bottom. In the equation, T is the temperature after exposure time t, T′ is the initial temperature and the temperature of the sample holder, q′ is the rate of heating in the Zircaloy-2, A is the heat transfer area of the Zircaloy-2 per unit weight, L is the thickness of air gap, K is the thermal conductivity of air, and C is the specific heat of Zircaloy-2.

Using the following values for the parameters,

$q' = 0.24$ cal,$\sec^{-1}$,g^{-1} (at 1 μamp)

$A = 3.8\ \text{cm}^2,\text{g}^{-1}$

$L = 0.022\ \text{cm}$

$C = 0.066\ \text{cal},\text{g}^{-1},{}^\circ\text{C}^{-1}$

$K = 5.7 \times 10^{-5}\ \text{cal},\text{sec}^{-1},\text{cm}^{-1},{}^\circ\text{C}^{-1}$

$T = 23^\circ\text{C}.$

The calculated wall temperature following 10 sec of irradiation is 42°C. During the same time, the calculated temperature rise in the solution is 3.8°C if it is again assumed that the heat was not exchanged between solution and walls. Now if it is assumed that the heat absorbed within the cell remains within the cell and is distributed to yield a uniform temperature, the uniform temperature rise is about 7°C. It was concluded that the temperature of the solution during irradiation at 1 μamp for 10 sec was below 35°C at the maximum. A more detailed calculation would be required to obtain the temperature more precisely. However, this was considered unnecessary since $G(Ce^{+3})$ does not change significantly with temperature below about 35°C.

Some experiments employed a current greater than 1 μamp. The calculated temperature changes for the largest current (2.27 μamps for 8 sec) were: (1) 39°C in the walls for the assumed condition that heat was transferred only to the mounting plate, (2) 7°C in the solution for the assumed condition that heat is not exchanged between solution and walls, and (3) 13°C for the cell assuming no heat exchange with surroundings but uniform distribution of temperature within the cell. The average solution temperature in this case was probably in the range for which $G(Ce^{+3})$ was 2.4 rather than the 2.5 prevailing below 35°C (Fig. IV.1).

The preliminary experiments to evaluate reduction of Ce^{+3} by reaction with cell walls were carried out using solution B in cell No. 1. Prior to these tests this cell had been irradiated while filled with solution B. The results of the tests showed that the Ce^{+4} was reduced at an average rate of 10^{-4} molar per hr during a 20 hr exposure at room temperature. Since the residence time during an experiment was 15 min, and the (Ce^{+4}) was determined with a precision of about 10^{-4} M, the average rate found in the control experiment indicated that reduction by the walls during an experiment was negligible. No control tests were made with 0.01 M Ce^{+4} solution since it was assumed that the reduction rate would not be increased by a reduction in (Ce^{+4}) concentration. This assumption was verified qualitatively by the observation that a solution which was initially 0.01 M Ce^{+4} still exhibited some ceric ion color after standing within cell No. 1 for 20 hr.

IV.5 Results

IV.5.1 Static Mock-up

The results of the series of dosimeter experiments with the static cell mock-up are listed in Table IV.8 together with germane experimental information and explanatory notes. The positions of the cell with respects to the Van de Graaff window and of the gold scatterer with respect to the cell duplicated those used in a previous experiment (Exp. 3, Appendix III, 2.27 cm between window and plane of coil, and 1 mil Au scatterer 0.48 cm from plane of coil). The series of experiments was completed during an 8-hr working period (9-29-65). The order of sample collection was the same as the order of listing. The beam

Tabel IV.8 Dosimetry Experiments with Static Cell Mock-up

Pertinent Experimental Information and Results

Sample No.	V.d.G. Run No.	Sample or Experiment Description	V.d.G. Exposure Time (sec)	Volume of Sample Collected (cc)	Average Flow Rate (cc/sec)	Residence Time in Beam[a] (sec)	Average Current[b] (µamp)	Current to Sample (µamp-sec)	(Ce^{+4}) (M)	(Ce^{+3}) (M)	Calculated Dose to Sample (ev/cc)	Calculated Dose Rate to Sample at 100 µamp[c] (w/cc)	Dose in Cobalt Source (min)	Dose in Cobalt Source (ev/cc H_2O)	$G(Ce^{+3})$ in Cobalt Source[e]
1	--	Sol'n placed in reservoir on 9/27/65	--	--	---	--	--	--	.00913	--	--	--	--	--	--
2	--	Fresh sol'n placed in reservoir on 9/29/65	--	--	---	--	--	--	.00995	--	--	--	--	--	--
2a	--	γ-ray test	---	--	---	--	--	--	.0055	.00445	--	--	82.4	$1.10x10^{20}$	2.33
3	1	--	90	14.5	0.161	.0720	81.0 (63-100)	5.83	.00745	.00240	$5.94x10^{19}$	164	--	--	--
4	2	Control Irradiation	90	14.0	0.156	0	78.4 (70-90)	--	.00985	--	--	--	--	--	--
5	3	--	120	13.0	0.108	.107	82.0 (75-95)	8.78	.0066	.00325	$8.03x10^{19}$	146	--	--	--
6	--	Control	--	18.6	0.103	0	--	--	.0095	--	--	--	--	--	--
7	4	--	110	12.5	0.114	.102	95.4 (95-100)	9.74	.0061	.00375	$9.26x10^{19}$	152	--	--	--
8	5	Control Irradiation	120	12.0	0.100	0	91.5 (64-100)	--	.00985	--	--	--	--	--	--
9	6	--	180	14.8	0.0819	.142	46.9 (43-100)	6.64	.00738	.00234	$5.78x10^{19}$	139	--	--	--
10	7	--	180	15.0	0.0833	.139	45.3 (24-49)	6.30	.00742	.00230	$5.70x10^{19}$	145	--	--	--
11	8	Control Irradiation	180	14.5	0.0806	0	47	--	.00972	--	--	--	--	--	--
12	--	Control	--	13.9	0.0772	0	--	--	.00972	--	--	--	--	--	--
12a	--	γ-ray test Sol'n from No. 12	--	--	--	--	--	--	.00432	.00540	--	--	93.6	$1.25x10^{20}$	2.49
13	9	--	360	27.75	0.0771	.151	16.7 (2-40)	2.52	.00889	.00083	$2.05x10^{19}$	131	--	--	--
14	10	--	600	10.5	0.0175	.663	14.6 (2-50)	9.66	.00589	.00308	$7.62x10^{19}$	126	--	--	---
15	11	Control	600	6.0	0.0100	0	15 (0.5-50)	--	.00897	--	--	--	--	--	--
16	12	Control Irradiation	600	6.0	0.0113	0	15 (10-35)	--	.00895	--	--	--	--	--	--
17	--	Control	--	7	0.0117	0	--	--	.0088	--	--	--	--	--	--
18	--	Control	--	20	0.1	--	--	--	.0095	--	--	--	--	--	--
18a	--	γ-ray test Sol'n from No. 18	--	--	---	--	--	--	.00447	.00503	--	--	90.3	$1.21x10^{20}$	2.40

a. Calculated assuming diameter of test tube equal to 22.6 mils.
b. Values in parentheses represent range of current during exposure.
c. A value of 2.44 for $G(Ce^{+3})$ was employed.
d. Evaluated from availabel calibration and relative γ-ray absorption coefficients in H_2O.
e. Temperature of solution in cobalt source was about 40°C.

current varied appreciably during some of the experiments, and the upper and lower values of the current are listed in addition to the average current.

The results of the control experiments showed that the general background of γ-rays prevailing during Van de Graaff operation did not affect the (Ce^{+4}) significantly. Some reduction of Ce^{+4} occurred during passage of the solution thru the tubing and during continued standing in the tank. The reference (Ce^{+4}) in a solution irradiation experiment was taken as that found in that control experiment which was carried out at about the same time and which employed the approximate flow rate used in the experiment. The average value for G(Ce^{+4}), 2.41 ± 0.08, compares favorably with the value of 2.40 ± 2-3% shown by the results at 40°C reported by Taimuty and coworkers.[13]

The values for the normalized power density from the experiments at 45 μamps and above are in reasonable agreement. Those obtained from the experiments at approximately 15 μamps are significantly lower. However, one of the low current experiments, No. 9, should be disregarded because, owing to a high flow rate, the fraction of Ce^{+4} reduced was only about 0.1. As previously mentioned, the validity of the dosimeter technique has not been established for a fractional reduction of less than 0.2. The control concentration of Ce^{+4} for the other low dose rate experiment, No. 10, was not satisfactorily established, and hence the uncertainty in this result is greater than that for the other, higher dose rate, experiments. Also, as mentioned previously any uncertainty resulting from low velocity regions in the cell is most pronounced at the lowest velocity.

The evaluation then is that the results show a normalized dose rate to the solution of 149 w/cc with a standard error of 4.2 w/cc (± 5.0 w/cc at 70% confidence) corresponding to the scatter of the high power density data. Including the uncertainty in the value of G(Ce^{+3}) which is indicated by the scatter of the experimental values for G(Ce^{+3}) in Table IV.8, the overall estimated error at 70% confidence is ± 12 w/cc.* The value of 149 w/cc in solution corresponds to 145 w/cc in water (Sec. IV.3.3).

IV.5.2 Dynamic Mock-up

The results of the experiments with the dynamic cell mock-up are listed in Table IV.9 together with experimental information and notes. As previously mentioned, the control samples were not placed within the cell. A determination of G(Ce^{+3}) for the solution gave a value of 2.45. A special effort was made to assure electrical contact between cell and mounting plate for Exps. 7 and following ones by clamping one tube to the mounting plate with an alligator clip. With earlier experiments, the cell was simply set in place.

The results of the dosimetry experiments scattered appreciably, and two results were greatly out of line on the low side. Possible explanation for this scatter include: (1) analytical errors with the small samples, and (2) errors resulting from poor electrical contact between cell and mounting plate. A poor electrical contact would result in a low dose rate since charges collecting on the cell would repel electrons. Within the uncertainty in the results, there was no effect of the changes in window thicknesses, backscattering material, or distance of standoff of the electron scatterer. Neglecting the two out-of-line and low values, the average normalized power density in the solution was 158 w/cc with a standard error of 6.9 w/cc (± 7.6 w/cc at 70% confidence) corresponding to the scatter of the data. Including the uncertainty

---

*The method employed in these estimates was an adaptation of that described by M. A. Kastenbaum, Biometrics, 15, 323, 1959.

Table IV.9 Dosimetry Experiments with Dynamic Cell Mock-up

Pertinent Experimental Information and Results

Experiment No.	Cell No.	Thickness Window	Thickness Back	Distance from V.d.G. Window to Cell Window	Standoff of Scatterer	Voltage	Average Current[d]	Length of Irradiation	Total Current	Back-scatterer	Concentration of Ce^{+4}	Concentration of Ce^{+3}	Calculated Dose Rate to Sample at 100 µamp[a]
		(mils)		(cm)	(cm)	(mev)	(µamp)	(sec)	(µamp-sec)		(M)	(M)	(w/cc)
1a	Control, no irradiation			-	-	-	-	-	-	-	.0098	-	-
1	1	3	20	2.9	.32	1.95	.338 (.2-1.1)	20.0	6.76	Zr-Brass	.0065	.0034	196
2	1	3	20	2.9	.32	2.00	.823 (.7-1.3)	12.0	9.88	Zr-Brass	.0064	.0035	137
3	1	3	20	2.9	.32	2.00	.616 (0-1.1)	15.0	9.24	Zr-Brass	.0084	.0015	63
4	1	3	20	2.9	.32	2.00	1.40 (1.0-1.9)	8.0	11.20	Zr-Brass	.0055	.0044	153
5	Control, no irradiation			-	-	-	-	-	-	-	.0095	-	-
6	1	3+7	20	2.9	.32	2.00	.961 (.92-.98)	10.0	9.61	Zr-Brass	.0059	.0040	162
7c	1	3	20	2.9	.32	2.00	1.42 (1.2-2.2)	7.0	9.94	Zr-Brass	.0058	.0042	164
8	Control, no irradiation			-	-	-	-	-	-	-	.0102	-	-
9c	1	3	20	2.9	.48	2.10	.696 (.2-1.2)	12.0	8.35	Zr-Brass	.0086	.0013	60
10c	2	3	20	2.9	.48	2.0	2.269 (1-4)	8.0	18.2	Zr-Brass	.0034	.0065	144[b]
16c	2	11	3	2.9	.48	1.95	.873 (.5-2)	15.0	13.1	63 mil Pb	.0041	.0052	153
17	Control, no irradiation			-	-	-	-	-	-	-	.0100	-	-
18c	2	11	3	2.9	.48	1.95	1.09 (.7-2.3)	9.0	9.81	63 mil Pb	.0066	.0033	130
19c	2	11	3	2.9	.48	2.00	.810	8.0	6.48	Brass	.0070	.0029	174

a. A value of 2.48 for $G(Ce^{+3})$ was employed.
b. A value of 2.40 for $G(Ce^{+3})$ was employed.
c. Care taken to assure contact between cell and plate
d. Values in parentheses represent range of current during exposure.

in the value of $G(Ce^{+3})$ which is indicated by the scatter of experimental values for $G(Ce^{+3})$ in Table IV.8, the overall estimated error at 70% confidence is ± 23 w/cc.* The value of 158 w/cc in the solution corresponds to 153 w/cc in water (Sec. IV.3.3).

IV.6 Conclusions

IV.6.1 Static Cell

The results of dosimetry measurements at 45 to 95 μamps are considered to be reliable values for the dose rate in the mock-up at these and other beam currents. The lowest dose rate in these particular experiments was a factor of three greater than that for which the validity of the dosimetry technique has been previously established. However, theoretical considerations revealed no reason to question the validity of the dosimetry technique at these higher dose rates. The results show that a power density of 145 w/cc at 100 μamps can be readily achieved. Furthermore, since the mock-up design was very similar to that of the experimental cell, it was possible to closely estimate the power density in a similarly positioned experiment from these mock-up results.

IV.6.2 Dynamic Cell

The dosimetry experiments indicate that a fairly uniform** power density of about 150 w/cc at 100 μamps can be achieved in the proposed dynamic cell without the use of special backscattering material. The proposed cell design will differ sufficiently from the mock-up design that it will be worthwhile to perform additional dosimetry experiments in which the ceric solution is exposed within the cell. The expected precision of the measurements using the experimental cell will be greater than that in the mock-up because of the greater solution volume and greater dose rates which can be employed.

---

*The method employed in these estimates was an adaptation of that described by M. A. Kastenbaum, Biometrics, 15, 323, 1959.

**The existence of a nearly uniform power density was deduced from previously reported results for the uniformity of the beam current for the cell and scatterer positions used in the dosimetry experiments (Exp. 8 of Appendix III, 2.91 cm window separation with 1 mil Au separated from the cell by 0.48 cm).

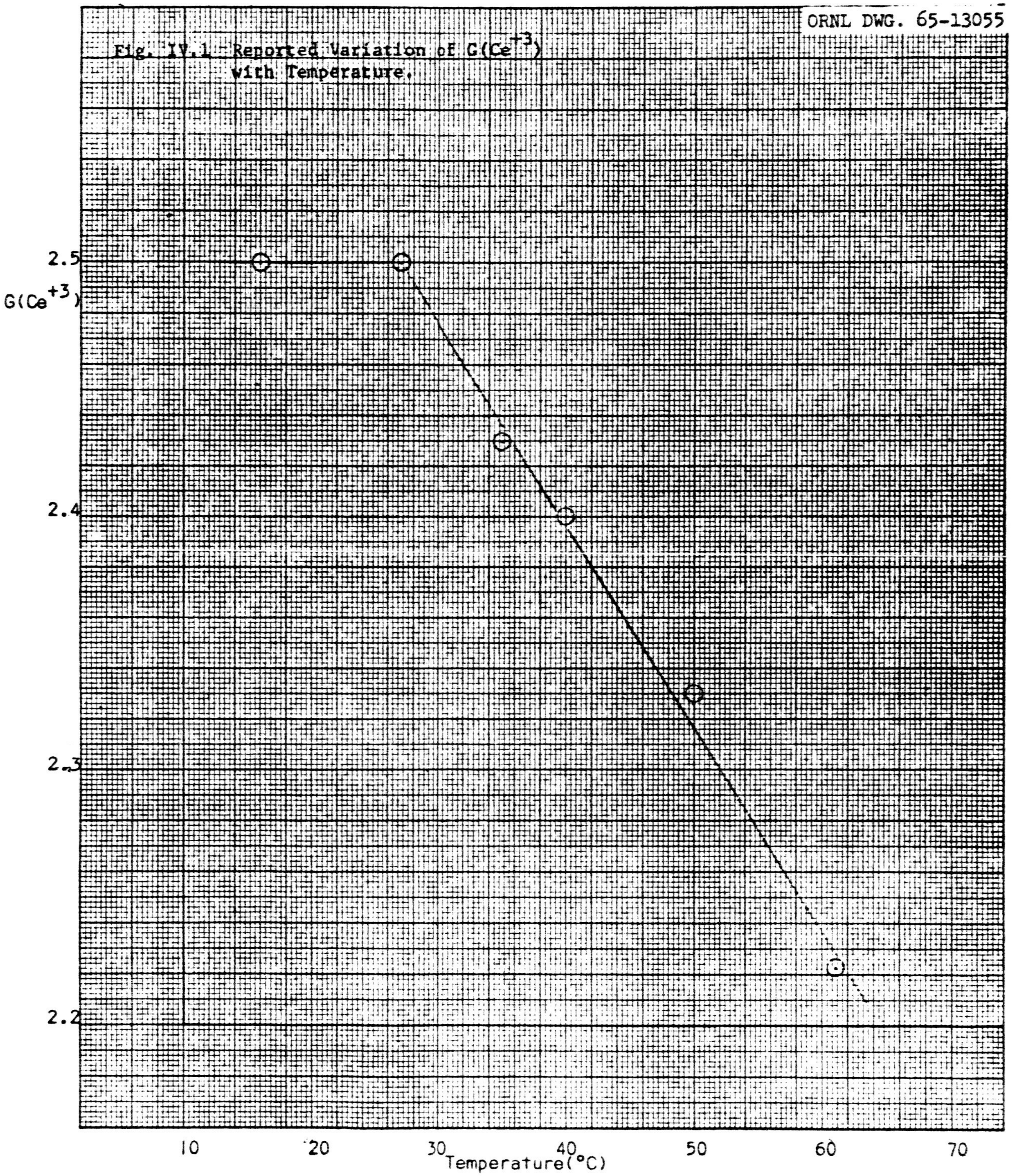

ORNL DWG. 65-13055

Fig. IV.1 Reported Variation of $G(Ce^{+3})$ with Temperature.

PHOTO 81631

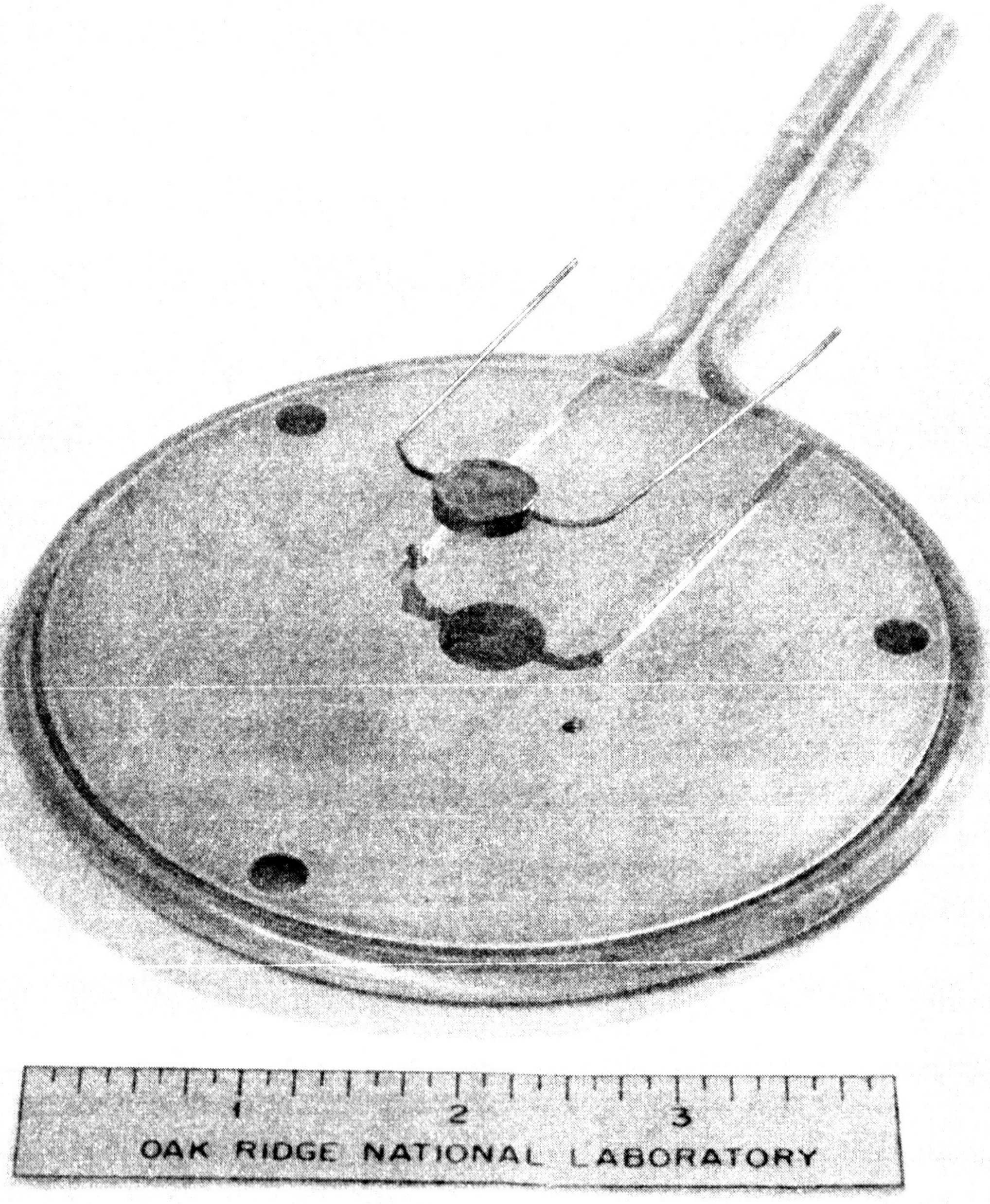

Fig. IV.2. Dynamic Mock-Up Cell and Mounting Plate.

Appendix V

Fabrication of Cell and Jacket Assembly

A length of Zircaloy-2 tubing (~3 in.) was chemically polished on internal surfaces to produce an ID of about 25 mils. A 0.8 in. length at one end was polished further to an ID of 26 to 27 mils. (This enlargement was made for accommodation of the filter). This tube was annealed at 700°C in a stream of He for a few min, after which it was inserted into the stainless steel jacket tubing using copper shim stock to insure proper separation between the two tubes. The loop was formed, and the tubes reannealed at 700°C. The copper shim stock was then dissolved in HNO_3. An additional 1 mil was then removed from the ID by chemical polishing. In some cases, tests were made of adsorption of Cd at room temperature on this final surface. The filter was then fabricated and forced into the enlarged section of the tubing, and the assembly was x-rayed in order to check tube separation and filter position. Final assembly of the equipment was carried out.

Appendix VI

Invalid Radiation Experiments

The analytical results of several consecutive experiments showed marked variations between the concentrations of Cd in solutions sampled at different times, (Table VI.1). The nature of the variations - the difference between samples taken at about the same time was less than that between those taken before and after appreciable amounts of solutions were passed through the system, duplicate samples of reservoir solutions were in reasonable agreement, and the variations in concentrations were on the high side of the expected ones - led us to believe that the variations resulted from deposition of Cd-bearing solids at some location within the solution system other than the cell or downstream tubing. Assuming that this was the case, the variations would be explained by assuming that more or less Cd was redissolved by the solution which was passed during the flush which followed the acid flush of the cell. These results were therefore considered invalid and were disregarded in stability evaluations.

Table VI.1

Non-Valid Experiments Conducted Using Cell-4 and 0.02 M $CdSO_4$ at 77°C

Date	Radiation Intensity (μamps)	Sample No.[a]	Amount of Cd in 10λ of Solution(μg)				
			Control		Radiation		Reservoir[d]
			A[b]	B[c]	A[b]	B[c]	
5/6	100	229-230	17.7	18.2			
		231-232			18.8	18.7	
		233-1					18.4
		233-2					18.2
5/10	66	234-235	21.5	20.4			
		236-1					18.8
		236-2					18.7
		237-238			19.8	18.0	
		239-1					17.0
		239-2					17.7
		240-241			17.0	18.1	
		242-1					19.4
		242-2					19.8
		243-244	17.3	17.6			
5/11	66	245-246	18.1	18.1			
		247-1					21.7
		247-2					21.7
		248-249			18.3	18.2	

a. Exposure time for control and radiation experiments was 30 min.

b. Sample of irradiated or control solution.

c. Sample of solution in cell at time irradiation or control was terminated.

d. Sample of reservoir solution collected in S and then placed in flask from which 10λ samples were withdrawn at a later time.

References

1. G. H. Jenks, E. G. Bohlmann and J. C. Griess, "An Evaluation of the Chemical Problems Associated with the Aqueous Systems in the Tungsten Water Moderated Reactor, Addenda 1 and 2," ORNL-TM-978, NASA-CR-54214, March 1965.
2. J. H. Baxendale and R. S. Dixon, Proceedings Chem. Soc., May 1963, p 148.
3. J. H. Baxendale, E. M. Fielden, and J. P. Keene, Proceedings Chem. Soc., August 1963, p 242.
4. J. H. Baxendale, Radiation Research, Supplement 4, 133 (1964).
5. G. E. Adams, J. H. Baxendale, and J. W. Boag, Proceedings Chem. Soc., August 1963, p 241.
6. A. O. Allen, "The Radiation Chemistry of Water and Aqueous Solutions," D. van Nostrand Co., Inc., Princeton, N. J., 1961.
7. L. M. Dorfman, *Science*, **141**, 493-498 (1963).
8. Ann T. Nelms, NBS Circular 577, July 1956.
9. A. Charlesby, "Atomic Radiations and Polymers," Pergamon Press, N. Y., 1960, p 32.
10. A. Chapiro, "Radiation Chemistry and Polymer Systems," Interscience, N. Y., 1961.
11. R. D. Birkhoff, *Handbuch der Physik*, Vol. **34**, 1958, pp 53-138.
12. K. A. Wright and J. G. Trump, "Back-scattering of Megavolt Electrons from Thick Targets," *J. App. Phys.*, **33**, 687 (1962).
13. S. I. Taimuty, L. H. Towle, and D. L. Petersen, *Nucleonics*, **17**, No. 8, 103-107 (1959).
14. J. W. Boyle, Oak Ridge National Laboratory, private communication.
15. J. T. Harlon and E. J. Hart, "Ceric Dosimetry: Accurate Measurements at 10^8 Rads," *Nucleonics*, **17**, No. 8, 102, 107-111 (1959).

16. G. Czapski, B. H. J. Bielski, and N. Sutin, J. Phys. Chem., 67, 201 (1963).

17. A. O. Allen, op.cit., p 38.

18. J. A. Ghormley and C. J. Hochanadel, Rad. Res., 3, 227 (1955).

19. A. O. Allen, op.cit., p 6 and p 54.

20. A. O. Allen, op. cit., p 47.

21. C. J. Hochanadel, Oak Ridge National Laboratory, private communication.

22. G. H. Jenks, H. C. Savage and E. G. Bohlmann, Oak Ridge National Laboratory, NASA Tungsten Reactor Radiation Chemistry Studies, Phase I, Experiment Design, ORNL-TM-1403, NASA-CR-54887, March 1966.

23. G. H. Jenks, H. C. Savage and E. G. Bohlmann, Oak Ridge National Laboratory, NASA Tungsten Reactor Chemistry Studies Monthly Progress Report for Period Ending April 30, 1966, ORNL-CF-66-6-7, July 6, 1966.

Internal Distribution

1. S. E. Beall
2. E. G. Bohlmann
3. G. E. Boyd
4. E. L. Compere
5. J. C. Griess
6. W. R. Grimes
7. C. J. Hochanadel
8. G. H. Jenks
9. C. E. Larson
10. F. L. Culler
11. H. F. McDuffie
12-13. A. J. Miller
14. H. C. Savage
15. M. J. Skinner
16. A. M. Weinberg
17-18. Central Research Library, Document Section
19. Y-12 Technical Library, Document Section
20-21. Laboratory Records Department
22. Laboratory Records Department (LRD-RC)
23. Reactor Division Library

External Distribution

24. S. G. English, U.S. Atomic Energy Commission,
Washington 25, D. C.
25. H. B. Finger, U.S. Atomic Energy Commission,
Washington 25, D. C.
26-30. Harry W. Davison, NASA
Lewis Research Center, 21000 Brookpark Rd., Cleveland, Ohio
31. L. V. Humble, NASA-Lewis Research Center
21000 Brookpark Road, Cleveland, Ohio 44135
32. S. J. Kaufman, NASA-Lewis Research Center
21000 Brookpark Road, Cleveland, Ohio 44135
33. M. H. Krasner, NASA-Lewis Research Center
21000 Brookpark Road, Cleveland, Ohio 44135
34. N. T. Musial, NASA-Lewis Research Center
21000 Brookpark Road, Cleveland, Ohio 44135
35. J. E. Morrissey, U.S. Atomic Energy Commission,
Washington 25, D. C.
36. H. M. Roth, U.S. Atomic Energy Commission,
Oak Ridge, Tennessee
37. J. C. Liwosz, Jr., NASA-Lewis Research Center
21000 Brookpark Road, Cleveland, Ohio 44135
38-39. LIBRARY, NASA-Lewis Research Center
21000 Brookpark Road, Cleveland, Ohio 44135

40. Report Control Office, NASA-Lewis Research Center
21000 Brookpark Road, Cleveland, Ohio 44135

41-46. NASA Representative, NASA Scientific and Technical
Information Facility
Box 5700
Bethesda, Maryland

47-49. U. S. Atomic Energy Commission
Technical Reports Library
Washington, D. C.

50-64. U. S. Atomic Energy Commission
Technical Information Service Extension
P. O. Box 62
Oak Ridge, Tennessee

65-66. W. F. Eanes, Westinghouse Electric Corporation
Atomic Power Division
Box 355
Pittsburgh, Pa.

67. Research and Development Division, ORO